

RESEARCH ARTICLE

10.1002/2013WR014420

Key Points:

- Meadow and watershed properties influence meadow response to stream channel incision
- Postincision streamflow change is influenced by changes in the groundwater system
- Postincision streamflow change is sensitive to change in evapotranspiration

Correspondence to:

H. I. Essaid,
hiessaid@usgs.gov

Citation:

Essaid, H. I., and B. R. Hill (2014), Watershed-scale modeling of streamflow change in incised montane meadows, *Water Resour. Res.*, 50, 2657–2678, doi:10.1002/2013WR014420.

Received 12 JULY 2013

Accepted 22 FEB 2014

Accepted article online 27 FEB 2014

Published online 25 MAR 2014

Watershed-scale modeling of streamflow change in incised montane meadows

Hedeff I. Essaid¹ and Barry R. Hill²

¹U. S. Geological Survey, Menlo Park, California, USA, ²U. S. Department of Agriculture—Forest Service, Vallejo, California, USA

Abstract Land use practices have caused stream channel incision and water table decline in many montane meadows of the Western United States. Incision changes the magnitude and timing of streamflow in water supply source watersheds, a concern to resource managers and downstream water users. The hydrology of montane meadows under natural and incised conditions was investigated using watershed simulation for a range of hydrologic conditions. The results illustrate the interdependence between: watershed and meadow hydrology; bedrock and meadow aquifers; and surface and groundwater flow through the meadow for the modeled scenarios. During the wet season, stream incision resulted in less overland flow and interflow and more meadow recharge causing a net decrease in streamflow and increase in groundwater storage relative to natural meadow conditions. During the dry season, incision resulted in less meadow evapotranspiration and more groundwater discharge to the stream causing a net increase in streamflow and a decrease in groundwater storage relative to natural meadow conditions. In general, for a given meadow setting, the magnitude of change in summer streamflow and long-term change in watershed groundwater storage due to incision will depend on the combined effect of: reduced evapotranspiration in the eroded meadow; induced groundwater recharge; replenishment of dry season groundwater storage depletion in meadow and bedrock aquifers by precipitation during wet years; and groundwater storage depletion that is not replenished by precipitation during wet years.

1. Introduction

Montane meadows are generally locations of groundwater (GW) discharge to streams in the mountain ranges of the western United States [Lord *et al.*, 2011; Jin *et al.*, 2012; Payn *et al.*, 2012]. Fryjoff-Hung and Viers [2013] surveyed 112 meadows throughout the Sierra Nevada and reported that 27% of the meadows were headwater sources of streamflow, only 4% were sinks for surface-water inflows, and an additional 46% had through-flowing streams. These groundwater-dependent meadows provide important ecosystem services including specialized habitat and vegetation; buffering of water, chemical and sediment fluxes; and GW storage for downstream supplies [Boulton, 2005; Murray *et al.*, 2003; Orellana *et al.*, 2012]. Development and land use practices have caused channel incision and streambed lowering in many montane meadows [Ratliff, 1985; Chambers *et al.*, 2011]. This has resulted in lowering of GW tables and changes in the magnitude and timing of watershed and meadow fluxes. Loheide *et al.* [2009] presented a comprehensive framework for hydroecological conditions in wet meadows of the Sierra Nevada and Cascade Mountains based on several case studies. They concluded from their extensive work in meadow systems that meadow GW flow was influenced by the regional GW flow into the meadow, the meadow hydraulic properties, and the degree of stream incision. There is substantial interest on the part of the scientific community and water and land resource managers to better understand surface water (SW)-GW interactions within meadows, the change in meadow hydrodynamics in response to stream incision and restoration, and the net effect of stream channel incision and restoration on watershed streamflow.

Field studies have been conducted to characterize the changes in streamflow, GW conditions, and water balances caused by meadow stream channel incision and restoration. Tague *et al.* [2008] evaluated the change in streamflow gain within a section of Trout Creek, California, prior to and after stream channel restoration. They observed that restoration led to less streamflow during the early part of the snowmelt recharge season and hypothesized that this was due to enhanced storage of water in the riparian zone due to enhanced recharge and overbank flows. They observed increased streamflow gain during the recession

period following peak snowmelt recharge under restored natural conditions and hypothesized that this was due to drainage of the riparian GW system. During the summer and early fall, there was little difference between pre and postrestoration flows.

Field studies examining GW conditions and meadow water balances have been conducted in relatively undisturbed montane meadows [Allen-Diaz, 1991; Sanderson and Cooper, 2008; Lord et al., 2011] and in incised and restored meadows [Loheide and Gorelick, 2005, 2006, 2007; Klein et al., 2007; Tague et al., 2008; Hammersmark et al., 2008, 2009; Loheide et al., 2009]. These studies have documented the influence of hydrologic setting and hydraulic properties on meadows; the close relationship between water table depth and vegetation patterns; the reliance of vegetation on the availability of shallow GW during the dry summer months; and the relationship between water table depth and GW evapotranspiration.

Determining the net effect of channel incision and restoration on streamflow and meadow hydrology in the field is challenging because studies comparing natural and incised meadows often are impacted by temporal climate variability, and/or spatial variability in conditions along stream reaches or between meadows. Models are useful tools for systematically simulating hydrologic conditions under both natural and incised conditions. Numerical modeling of incised and natural/restored conditions can be used to systematically study the impacts of channel incision on the hydrodynamics and water balances for a range of meadow settings. Many modeling methods have been used to simulate meadows including variably saturated flow, saturated flow, distributed and lumped parameter, and coupled hydrologic models [Orellana et al., 2012].

GW-based modeling studies, incorporating increasing sophistication of SW representation, have provided considerable insight into meadow hydrology. Wood [1975] examined meadow water table configurations under different GW inflows and evapotranspiration (ET) demands to understand the hydrologic conditions required for development of a wet meadow. Loheide and Gorelick [2007] showed that stream incision caused a shift to drier vegetation near the stream channel due to the lowered water table, while margins of the meadow away from the stream continued to support wet meadow vegetation. Loheide et al. [2009] examined the effect of hydraulic properties and varying proportions of lateral and basal inflow on meadow water table configuration. Their results indicated that wet meadow conditions were favored by lower hydraulic conductivity meadow sediments, higher GW inflow rates, and a higher ratio of lateral to basal GW inflow. They also showed that stream incision under these conditions had relatively little impact on the margins of the meadows where wet conditions were sustained. Lowry et al. [2010] improved the analysis of meadow hydrodynamics by incorporating the time-varying snow-melt-derived GW influx to the meadow into a model of Tuolumne Meadows, CA. They concluded that including the temporal variability of hillslope inflow was important for understanding water table dynamics in montane meadows. Lowry et al. [2011] extended this work to include the effect of stream stage fluctuation, and Loheide and Booth [2011] examined the influence of channel morphology on meadows. Lowry and Loheide [2010] used unsaturated zone flow modeling to show that meadow ET occurs from moisture held in the shallow fine-grained soil zone (SZ) and directly from the water table. They identified a GW sustained component of ET termed "the GW subsidy" that represents ET from saturated GW as opposed to ET from moisture held in the draining SZ. Field studies by Sanderson and Cooper [2008] documented the importance of GW ET and estimated that it was 75–88% of total annual ET in wet meadows.

Watershed models that couple climate conditions, multiple streamflow generation processes, and a relatively simplified representation of the GW flow system (compared to comprehensive GW flow models) have been used to study meadows. Hammersmark et al. [2008, 2010] modeled incised and restored stream channel conditions in a 2.6 km² montane meadow along a 3.6 km stretch of Bear Creek, CA. Their results showed that following restoration of the stream channel GW levels rose and GW storage increased; total annual watershed runoff decreased (by 1–1.6%); total annual ET increased (by 25–50%); flood peaks decreased; and base flow decreased in the meadow but increased downstream of the meadow. Ohara et al. [2013] simulated the 250 km² Last Chance watershed and examined the response to 13 km of stream channel restoration in a headwaters meadow. By comparing prerestoration and postrestoration simulations for the same climate conditions, they found that flood peaks decreased by 10–20% and base flow increased by 10–20% as a result of stream restoration.

These field and modeling studies have illustrated that meadow hydrology is determined by meadow hydraulic properties, lateral and basal GW inputs, surface inflows, vegetation and ET patterns, and stream

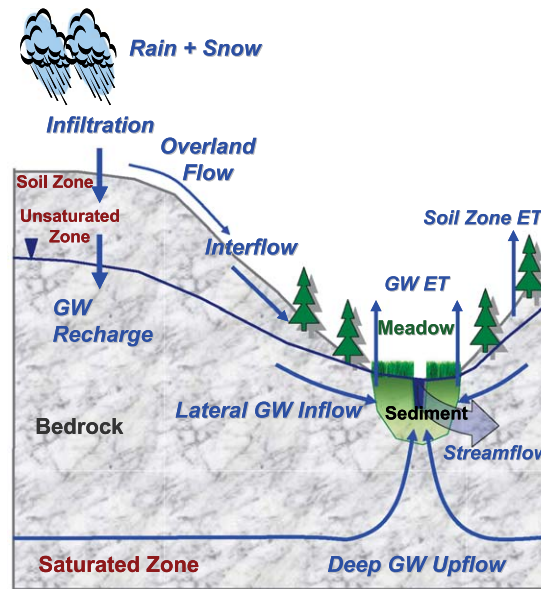


Figure 1. Conceptual model of coupled surface water-groundwater flow in a montane meadow watershed.

stage and channel morphology. SW and GW inflows to the meadow come from the encompassing watershed, and the dynamic nature of these flows is best characterized by simulating the entire watershed-meadow system. This study expands on previous modeling efforts by presenting the results of coupled SW-GW modeling of meadow hydrology within the encompassing watershed flow system that includes bedrock GW inflow and hillslope OF+IF to the meadow, SW-GW interactions in the meadow, SZ and GW ET, and the influence of changes in meadow water table on the adjacent hillslope and bedrock flow system. The model is used to contrast watershed and meadow hydrodynamics for a natural stream channel (representing preincision or postrestoration conditions) with incised stream channel conditions. Model results are used to compare the spatial patterns and seasonal trends in water table depth, streamflow, ET, and GW storage within the watershed and meadow

for natural and incised stream channels to provide a comprehensive understanding of the effect of stream incision on watershed and meadow hydrology.

2. Model Approach and Framework

The hydrology of montane meadows under natural and incised stream channel conditions has been investigated using the U.S. Geological Survey (USGS) coupled SW-GW flow model (GSFLOW) [Markstrom *et al.*, 2008], an integration of the USGS Precipitation-Runoff Modeling System (PRMS) [Leavesley *et al.*, 1983, 2005], and the USGS Modular Ground-Water Flow Model (MODFLOW) [Harbaugh, 2005]. Drying and rewetting of subsurface model cells due to water table fluctuations is facilitated by the Newton formulation for MODFLOW-2005 [Niswonger *et al.*, 2011]. GSFLOW was developed to simulate watershed-scale coupled SW and GW flow by simultaneously simulating flow across the land surface and within the subsurface. This modeling approach facilitates representation of the dynamic flow processes important for understanding meadow hydrology (Figure 1). Processes represented in this model include daily: rain, snowfall, and snowmelt; canopy interception and ET; streamflow, overland runoff, interflow, and infiltration; soil-zone storage and ET; vertical unsaturated zone (UZ) flow and ET, and GW flow and ET.

GSFLOW iteratively couples daily overland flow (OF) and streamflow across the land surface, interflow (IF) through and infiltration from the near-surface SZ, vertical flow through the unsaturated zone, and three-dimensional GW flow in the saturated zone. Water entering the SZ is first allocated to immobile pore water that can evaporate and transpire (stored in the fraction of the pore space represented by field capacity minus wilting point) with the excess becoming mobile pore water that can flow laterally and/or drain vertically to the unsaturated zone (stored in the fraction of the pore space represented by porosity minus field capacity). Climate data and watershed characteristics are used to compute daily precipitation (rain and/or snow), snowmelt and potential ET throughout the watershed. Actual ET depends on the availability of water and is the sum of snow sublimation (when snow is on the ground), ET from water intercepted and stored in the plant canopy and ET from water stored in the soil zone (SZ ET). If potential ET demand is not satisfied then ET occurs from the unsaturated zone (UZ ET) and GW zone (GW ET) if plant root depth reaches the water table. For simplification, capillary rise is neglected and GW ET is assumed to decrease linearly with water table depth ending when the water table falls below the root zone. Soil zone water is replenished by infiltration that may originate from direct precipitation or snowmelt, upslope OF+IF or GW seepage to the land surface. Overland flow is generated when the SZ is fully saturated, rainfall/snowmelt exceeds

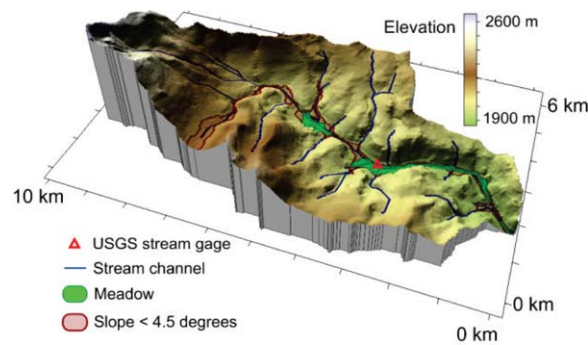


Figure 2. Configuration of the Sagehen watershed used to develop the model framework. Meadow regions delineated in green correspond to areas mapped as AQB—Aquolls and Borolls, 0–5% slope, in the SSURGO soil survey of the area (NRCS, USDA). The zone delineated in red (land surface slope <4.5°) was filled with alluvial sediment in the model and represented potential areas for meadow development.

infiltration capacity, and/or GW discharges to the land surface. Overland flow and inter-flow are routed toward stream channels based on land surface elevation and slope using a cascade procedure [Henson *et al.*, 2013]. Exchange of water between the stream and GW is dependent on streambed properties and the difference between stream stage and GW head. The simulated watershed must be discretized into Hydrologic Response Units (HRUs) for surface and SZ computations, a finite-difference grid for GW flow computations, and a stream network for streamflow routing.

2.1. Watershed Framework

A reference case (RC) watershed model was developed based on properties of a Sierra

Nevada watershed encompassing GW fed meadows. The Sagehen Creek watershed (Figure 2), located on the east slope of the northern Sierra Nevada near Truckee, California, USA, was used as the basis for the climate, topography, hydrography, vegetation, and soil properties of the modeled area. Considerable watershed information was available from work at the Sagehen Creek Field Station (<http://sagehen.ucnrs.org/>) and Experimental Forest (<http://www.fs.fed.us/psw/ef/sagehen/>), the USGS gage station summary of Mast and Clow [2000], the geologic map of Sylvester [2008], the Natural Resources Conservation Service (NRCS) of the United States Department of Agriculture (USDA) Soil Survey Geographic (SSURGO) Database, studies of Allen-Diaz [1991], Rademacher *et al.* [2005], Sylvester [2008], and Manning *et al.* [2012], and an existing GSFLOW model for the USGS gage station contributing area [Niswonger *et al.*, 2006; Markstrom *et al.*, 2008].

The Sagehen Creek area is characterized by cold wet winters and warm dry summers, and has a mean annual precipitation near the USGS gage of 85 cm with 82% in the form of snow [Manning *et al.*, 2012]. The modeled area of Sagehen Creek watershed is 37 km² and ranges in elevation from 1872 to 2653 m. The upper part of the basin is steep, whereas the lower part has a broad, U-shaped valley characteristic of glaciated terrain and meadow areas have developed adjacent to the stream (Figure 2). The observed meadow region (0.84 km²) delineated in Figure 2 corresponds to areas mapped as AQB—Aquolls and Borolls, 0–5% slopes in the SSURGO soil survey (Natural Resources Conservation Service, NRCS) of the area. Meadows in the Sagehen watershed are relatively undisturbed and still in their natural state (no incision). They are wet meadows fed by upslope inflows, as is characteristic of many Sierra Nevada meadows [Weixelman *et al.*, 2011; Viers *et al.*, 2013; Fryjoff-Hung and Viers, 2013], and discharge to Sagehen Creek in the valley floor. Flow in the creek is strongly influenced by snowmelt with peak flows in late spring (mean May discharge = 2.2 m³/s), minimum flows in the fall (mean October discharge 0.04 m³/s), and an average annual runoff of 40 cm from 1954 through 1995 [Mast and Clow, 2000].

Tertiary volcanic rocks (primarily andesitic lava flows, volcanoclastic deposits, and Pleistocene basalt) overlie Cretaceous granodiorite in the Sagehen watershed [Sylvester, 2007]. Pleistocene glacial deposits, colluvium, and alluvium cover much of the bedrock in the Sagehen Creek basin. SSURGO (NRCS) soil properties were used to estimate the hydraulic conductivity (K) and specific yield (S_y) for the top meter of soil (Table 1 and Figures 3a and 3b). Soil properties in the meadow zones were not available from the SSURGO database, but were estimated based on literature values and field tests [Earman *et al.*, 2013] to be K = 0.2 m/day and S_y = 0.2. Vegetation in the basin is primarily pine and fir forest with grassy meadows along the main channel. Lidar determined canopy height (UC Berkeley Center for Forestry lidar data coverage analyzed by National Center for Airborne Laser Mapping, retrieved from Sagehen Field Station Website: <http://sagehen.berkeley.edu/gis.htm> on 21 March 2011) was used to classify vegetation for modeling purposes as tree (>2 m), shrub (1–2 m), and grass (<1 m) with the resulting distribution shown in Figure 3c.

The observed thickness of alluvial surficial deposits ranges from a few meters or less near hillslopes to >15 m near the creek at lower elevations [Earman *et al.*, 2013]. Land surface slope (Figure 3d) was used to

Table 1. Select Model Parameters

Model Parameter	Value or Range
<i>Soil Zone</i>	
Soil zone thickness (szthick)	0.75 m
Porosity = 1 - (SSURGO soil bulk density/2.65)	0.45-0.68
Field capacity from SSURGO	0.06-0.25
Wilting point from SSURGO	0.02-0.14
Soil saturated hydraulic conductivity (K_{sat}) from SSURGO	0.2-2.4 m/day, Figure 3a
Land surface slope (slope)	Figure 3d
Maximum amount of water that can be stored in the soil zone = sat_threshold in GSFLOW = (porosity - wilting point)*szthick	0.25-0.48 m/m ²
Maximum amount of water that can be held in the soil zone by capillary forces = soil_moist_max in GSFLOW = (field capacity - wilting point)*szthick	0.02-0.08 m/m ²
Linear flow-routing coefficient = slowcoef_lin in GSFLOW = 0.5*slope*K _{sat} /((porosity - field capacity)*szthick)	0.001-1.23 day ⁻¹
Linear gravity drainage coefficient = ssr2gw_rate in GSFLOW = 0.01*K _{sat} /((porosity - field capacity)*szthick)	0.01-0.1 day ⁻¹
<i>Subsurface Zone</i>	
Thickness of alluvial sediments = (0.085 - land surface slope)/0.085*20	1-20 m
Depth = average depth of model layer	1-150 m
S _y at the land surface = porosity - field capacity	0.2-0.6, Figure 3b
RC meadow K = K _{sat} *(Depth) ^{0.9}	Figure 5a
RC bedrock K = K _{sat} *(Depth) ^{-0.9}	Figure 5a
RC meadow S _y = K _{sat} *(Depth) ^{0.15}	Figure 5b
RC bedrock S _y = K _{sat} *(Depth) ^{-0.3}	Figure 5b
BR+ meadow K = K _{sat} *exp(0.15*Depth)	Figure 5a
BR+ bedrock K = K _{sat} *exp(-0.06*Depth)	Figure 5a
BR+ meadow S _y = K _{sat} *exp(0.03*Depth)	Figure 5b
BR+ bedrock S _y = K _{sat} *exp(-0.06*Depth)	Figure 5b
Specific storage	1 × 10 ⁻⁶ m ⁻¹
Brooks-Corey exponent	1
ET extinction depth = Root depth	Grass = 0.5 m, Shrubs = 1.0 m, Trees = 2.0 m
<i>Stream Network</i>	
Stream segment flow accumulation (fac)	300-41345
Natural stream channel width = 0.5 + 4.9e-5*(fac-300)	0.5-2.5 m
Natural stream channel depth = 0.125 + 9.1e-6*(fac-300)	0.125-0.5 m
Extra incised width = (1 - (33557-fac)/(33557 - 15047))*6	0-6 m

estimate the zone of alluvial sediment accumulation and potential meadow development within the watershed. This 1.9 km² zone (Figure 2) was characterized as the area adjacent to the main branches of Sagehen Creek having land surface slope < 4.5° (0.08 m/m). Thickness of sediment in this zone (Figure 3e) was assumed to be proportional to slope (Table 1), ranging from 1 m at the hillslope margin of the alluvial zone to a maximum of 20 m in the flattest portion of the valley adjacent to the stream.

2.2. The Reference Case Model

The physical characteristics and climate of the relatively undisturbed Sagehen basin were used to specify realistic model parameters for the natural stream channel reference case simulation (RCnat); however, the RCnat model was not a rigorously calibrated simulation of the Sagehen watershed. The goal of the RCnat simulation was to develop a relatively parsimonious representation of a flow system that reproduced the general features observed in a Sierra Nevada watershed-meadow system under historical natural conditions. Simulations were conducted for water years 1980-1988 using observed daily temperature and precipitation records for Sagehen. Initial GW conditions were obtained from a steady state flow time step with an elevation-dependent average recharge distribution. This was then followed by a 9 year, daily-time-step transient simulation. Results for the first year of simulation (water year 1980) were not used in the analysis because they were influenced by the initial conditions in the soil zone. The results of the natural stream channel simulation were then compared to results from a simulation having an incised section of channel in the meadow area (Figure 4). The natural and incised simulations were conducted for the same time period, weather conditions, and initial steady state GW recharge distribution. Comparison of the results from these simulations provides insight into the difference in meadow hydrology and streamflow for established natural (or restored) and incised stream channels, but does not represent the period of transition from natural to incised conditions, or incised to restored conditions.

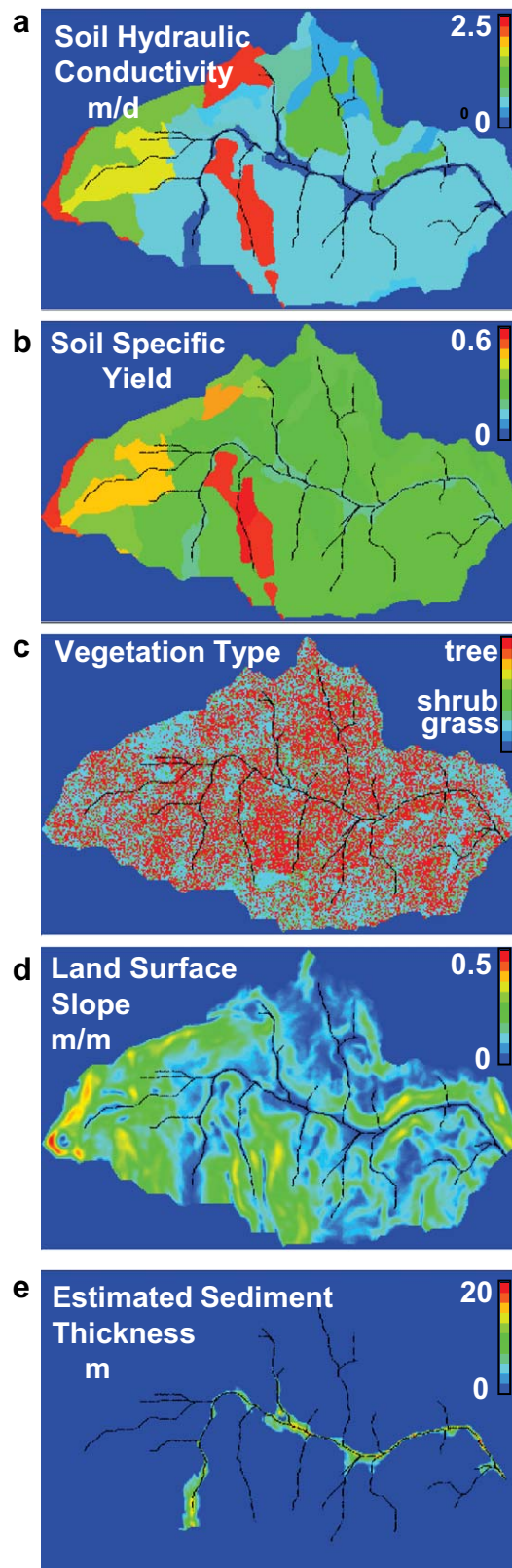


Figure 3. Sagehen watershed properties: (a) soil hydraulic conductivity, (b) soil specific yield, (c) vegetation type, (d) land surface slope, and (e) estimated alluvial sediment thickness.

The RC model draws on an existing two-layer GSFLOW model for the portion of Sagehen watershed contributing flow to the USGS gage [Niswonger *et al.*, 2006; Markstrom *et al.*, 2008]. The watershed area was enlarged and the horizontal and vertical watershed discretization refined (Figure 4). The simulated watershed outlet was placed well below the meadow areas so that boundary conditions would not influence meadow hydrology. Coinciding HRUs and MODFLOW grid blocks were discretized on a regular grid with 30 m square block size, to allow for ample spatial resolution in the meadow areas, resulting in 74,175 active grid blocks and HRUs. The 200 m thick subsurface GW system was discretized into nine layers ranging in thickness from 2 m (at the surface) to 105 m (bottom bedrock layer) facilitating representation of meadow stratigraphy.

In general, SZ and climate-related parameters were developed using the methods outlined at http://www.brr.cr.usgs.gov/projects/SW_MoWS/GSFLOW%20-%20Instructions%20for%20Input.html (accessed 11 January 2013). Parameters controlling SZ storage, infiltration from the SZ to GW, and OF+IF were estimated based on watershed properties (Table 1) with minor adjustment to reproduce the general streamflow pattern observed at the Sagehen USGS gage. The soil processes were simplified (to reduce the number of calibration parameters) by assuming a linear OF+IF flow-routing coefficient (GSFLOW parameter *slowcoef_lin* in Table 1) and a linear gravity-drainage coefficient (GSFLOW parameter *ssr2gw_rate* in Table 1) controlling infiltration from the SZ to GW. The values of SZ parameters were related to mapped soil properties and land surface slope (Table 1). Simulation results indicated that using this simplified approach to represent OF+IF processes with one parameter (i.e., neglecting nonlinear and fast OF+IF) was sufficient to reproduce the general flow characteristics of Sagehen Creek. Potential ET was calculated using the Jensen-Haise option in GSFLOW [see Markstrom *et al.*, 2008, p. 43] and is a function of air temperature and solar radiation. The model rooting depth distribution was based on the vegetation distribution (Figure 3c) with tree root depth = 2 m, shrub root depth = 1 m, and grass root depth = 0.5 m. These assumed maximum root depths were in accordance

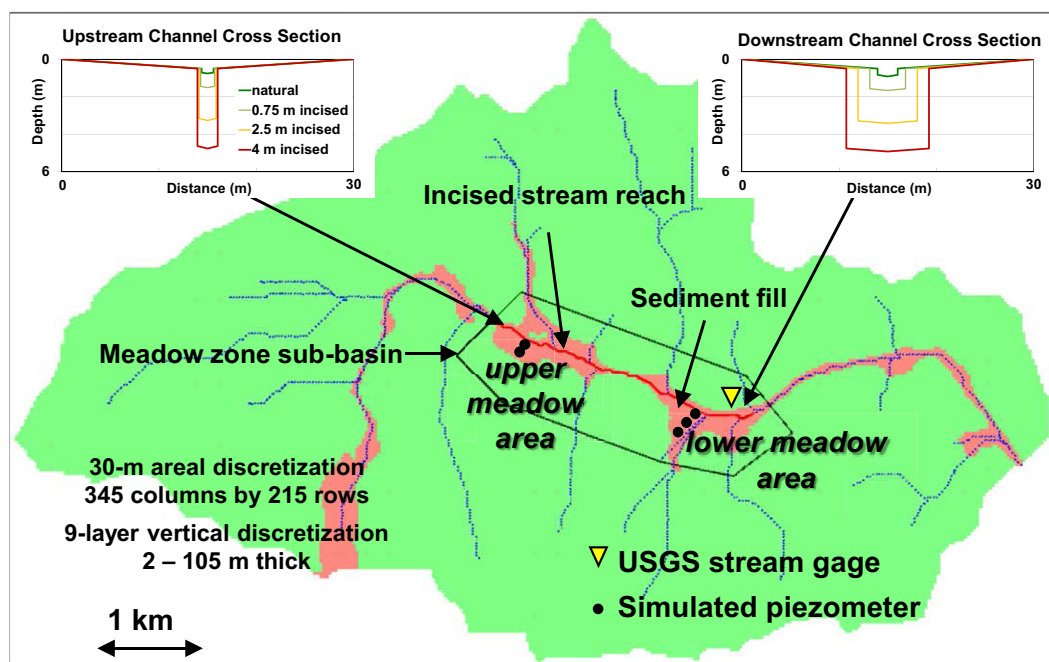


Figure 4. Model framework showing active model area (green), alluvial sediment-filled area (light red), meadow zone sub-basin area, stream network (blue), incised stream reach (red), upper and lower meadow areas, and stream cross sections for the beginning and end of the incised stream reach.

with the root depth distributions compiled by *Jackson et al.* [1996] for temperate coniferous forests, shrubs, and grassland.

The depth-dependent meadow hydraulic parameters were based on observations of Sierra Nevada meadow stratigraphy documented in the literature [*Wood, 1975; Loheide et al., 2009*], as well as well logs and pump test results from Sagehen [*Earman et al., 2013*]. Many Sierra Nevada meadows have low K fine-grained sediment and/or decomposed peat near the surface that transitions to higher K , coarser alluvial materials at depth believed to be deposited during past postglacial high flow periods. Pump test analysis [*Earman et al., 2013*] indicated that the K and S_y of alluvial sediments near Sagehen Creek ranged from about 0.2 m/day and 0.2, respectively, near the surface to >10 m/day and 0.3 at depth. The RC meadow K and S_y were represented with depth-dependent functions (Table 1) with K ranging from 0.2 m/day at the surface to a maximum of 2 m/day at depth (Figure 5a), and S_y ranging from 0.2 at the surface to a maximum of 0.3 at depth (Figure 5b). Bedrock K is known to decrease with depth [*Manning and Ingebritsen, 1999*], and *Jiang et al.* [2009] demonstrated that the rate of decrease with depth influences the local and regional GW flow patterns. In both studies, an exponential decay of K with depth was used to represent K in regional GW systems having a thickness >1 km. However, for this study, with its focus on the upper 200 m of the soil and bedrock system, simulations with a power-law decay (Table 1) gave a better fit for the Sagehen basin because the more rapid decrease in K at shallow depth better represented the rapid transition from soil and weathered bedrock to bedrock (Figure 5a). Depth-dependent bedrock S_y was handled in the same manner (Table 1 and Figure 5b) and specific storage was assumed constant and equal to $1 \times 10^{-6} \text{ m}^{-1}$.

The stream channel network (Figure 4) was determined by applying the flow accumulation tool of Arc Hydro [*Maidment, 2002*] and selecting the network of stream segments with flow accumulating from at least 0.027 km^2 (300 grid blocks). Each stream segment of the model was assigned a 30 m wide stream-floodplain cross section that included a distinct stream channel located within a gently sloping flood plain area. Stream channel width and depth were assumed to increase in proportion to stream flow. Flow accumulation values (FAC) for stream segments were used as a proxy for streamflow to relate the stream channel width and depth to cumulative flow (Table 1). Two examples of stream channel profiles within the stream network are shown in Figure 4. Under natural conditions, the stream channel width and depth increased from a minimum of 0.5 to 0.125 m (FAC = 300), respectively, at the headwaters of a stream reach

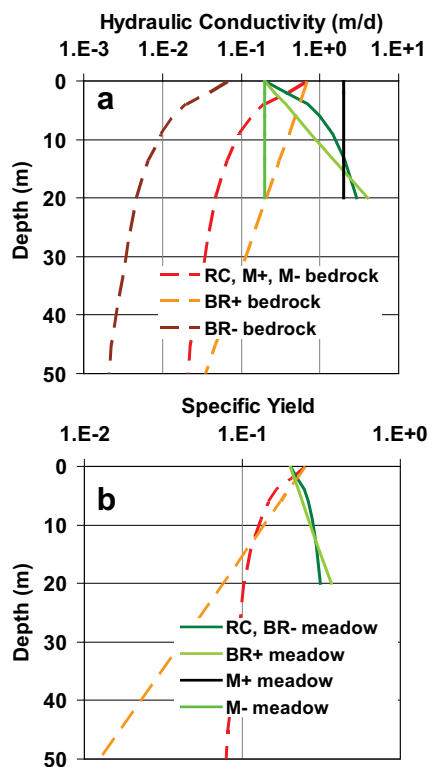


Figure 5. (a) Depth-dependent bedrock and meadow hydraulic conductivity and (b) specific yield used in model scenarios: RC reference case; BR+ increased bedrock hydraulic conductivity; BR- decreased bedrock hydraulic conductivity; M+ increased meadow hydraulic conductivity; and M- decreased meadow hydraulic conductivity.

to a maximum width and depth of 2.5 and 0.5 m (FAC = 41,345), respectively, at the outlet of the watershed. This stream channel configuration resulted in a close fit of the simulated rating curve to the observed rating curve at the USGS gage. During low streamflow periods flow was contained within the central stream channel, but during high streamflow the central channel became filled and flow extended over the flood plain portion of the stream cross section.

The 2.8 km stream reach subjected to incision (red stream segment in Figure 4) was contained within the area of the watershed encompassing the upper and lower meadow zones for the incised reference case simulation (RCinc). The uppermost end of the incised reach was located at a break in stream channel slope where the slope became shallower down valley. The lowermost end of the incised segment was located where the valley became constricted about 270 m downgradient from the USGS gage. The incision depth was tapered at the up valley and down valley ends of the incised stream reach so that the bottom of the incised stream channel would meet the undisturbed stream channel. The incised stream channel depth was obtained by increasing the natural stream channel depth by the amount of simulated stream incision (0.75, 2.5, and 4 m incision conditions were simulated). The incised stream width was assumed to be larger than the natural stream width, due to stream bank undercutting, and the widening was assumed to be proportional to streamflow and related to FAC (Table 1). Figure 4 shows incised stream channel profiles at upstream and downstream locations within the incised stream reach. As a result of stream incision, the stream channel becomes

deeper by the amount of incision; the channel remains narrow at the uppermost location but becomes progressively wider downstream as a result of incision and bank undercutting.

2.3. Modified Model Scenarios

Conditions in the RC watershed are characteristic of relatively wet hillslope and riparian meadows [as defined by Weixelman *et al.*, 2011]. Several scenarios with simple modifications to bedrock and meadow hydraulic properties, GW ET and postincision meadow root depth, and precipitation were simulated to broaden the spectrum of meadow conditions examined. The RC meadow comprised relatively high K meadow sediments at depth overlain by lower K material at the surface. However, meadow K may in some cases be lower than bedrock K [Hill and Mitchell-Bruker, 2010; Loheide *et al.*, 2010]. Depth-dependent bedrock and meadow K functions of the RC model were varied to create scenarios with different contrasts between bedrock and meadow K (Figure 5). The modified hydraulic conductivity scenarios were:

M- (Smaller Meadow K): The entire thickness of meadow sediment was assigned a uniform constant K (0.2 m/day) equal to the K of the surface layer of the RC meadow. Like the RC, the near-surface K of the meadow was less than that of the bedrock.

M+ (Larger Meadow K): The entire thickness of meadow sediment was assigned a uniform constant K (2 m/day) approximately equal to the K of the deepest meadow sediments of the RC case. SZ parameters dependent on near-surface K (GSFLOW parameters *slowcoef_lin* and *ssr2gw_rate* in Table 1) were adjusted to be consistent with this change in meadow surface K. This scenario represented a system with meadow K greater than bedrock K.

BR+ (*Larger Bedrock K*): Exponential depth-dependent K functions were used for the bedrock and meadow K. This resulted in a system with a more gradual decrease in bedrock K with depth (relative to the RC, Figure 5) allowing greater GW flow through the bedrock to the meadow.

BR- (*smaller bedrock K*): The bedrock K and gravity-drainage coefficient (GSFLOW parameter *ssr2gw_rate* in Table 1) outside of the meadow sediment area of the RC were reduced by an order of magnitude. This resulted in a system with meadow K greater than bedrock K and limited GW flow through the bedrock to the meadow.

GSFLOW differs from traditional watershed models in that it includes ET from GW tapped by roots. However, a limitation of GSFLOW is that it does not predict or adjust vegetation type (and root depth) based on water table depth. The RC-incised stream channel simulations were conducted with the root depth unchanged from the natural conditions. Two modified GW ET scenarios were considered:

RCnoGWET: ET from GW was turned off in this scenario and results compared to the RC to illustrate the role of GW ET.

RC0.5to2mRD: The observed vegetation distribution in Sagehen watershed (Figure 3c) was used to assign the root depth for the calculation of GW ET in the RC simulation. The observed Sagehen vegetation distribution resulted in root depths >0.5 m (the assumed root depth for meadow vegetation) in some of the potential meadow areas because of the presence of trees and shrubs. Thus, the natural stream RC simulation may overpredict GW ET. The RC-incised stream simulation was conducted with the natural condition root depth distribution unchanged, and did not represent the potential encroachment of vegetation having deeper tap roots such as trees, shrubs, and/or sagebrush following incision. Thus, the incised RC simulation may underpredict GW ET. In the *RC0.5to2mRD* scenario, the natural simulation root depth was 0.5 m in the meadow sediment area and the incised stream root depth was 2.0 m in the meadow sediment area. This scenario represented the transition from natural meadow vegetation to an incised system with complete invasion of deeper rooted vegetation.

Finally, one scenario of reduced precipitation was conducted to examine meadow hydrology in a drier watershed:

RC0.5PPT: The RC precipitation rate was reduced by one half.

The above underlined short form names are used in the discussions below. A “nat” suffix was applied to the short name for the natural stream simulation, and an “inc” suffix followed by the magnitude of incision (0.75, 2.5, and 4 m) was applied for the incised stream simulations. For example, *RCinc0.75m* refers to the reference case simulation with the stream channel incised by 0.75 m.

3. Reference Case Results

The natural stream (RCnat) simulation reproduced the general features observed in the Sagehen watershed confirming that the model was representative of a Sierra Nevada watershed-meadow system. Simulated streamflow at the USGS gage was close to the observed streamflow for most of the period of simulation (Figure 6). Simulated streamflow was greater during wet years (water year (WY) 82, 83, and 86) than during

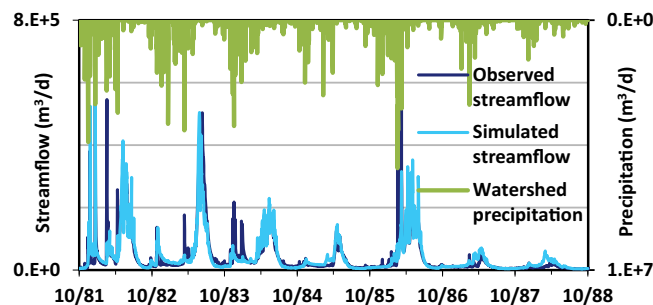


Figure 6. Watershed precipitation and RC observed and simulated streamflow at the USGS gage.

relative dry years (WY 85, 87, and 88) with streamflow peaks corresponding to periods of active snowmelt in the late spring/early summer. The timing and magnitude of the simulated snowmelt driven peaks corresponded to those observed in Sagehen. Streamflow peaks observed in Sagehen during the late fall and early winter (e.g., WY 82 and 84) caused by isolated rainfall and/or rapid snowmelt events were difficult to capture in the model. These peaks were reproduced in the

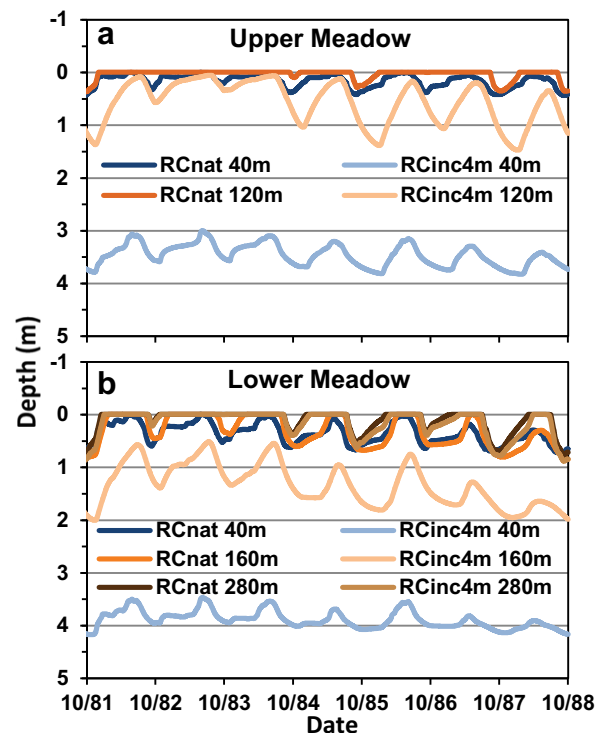


Figure 7. Simulated natural and 4 m incised water table depth histories at increasing distances from the stream channel for the (a) upper meadow area and (b) lower meadow area.

the seasonality of watershed fluxes (Figure 8a). Water was removed from the watershed via streamflow leaving the basin and ET from within the basin. SZ ET was the main ET component during the snowmelt season when the SZ remained moist. SZ ET began in spring and peaked between April and July depending on whether the year was dry (earlier peak) or wet (later peak). As the SZ dried out, GW ET from areas where the water table was within the root zone began to satisfy the potential ET demand. Annual GW ET was much less than SZ ET because the fraction of the watershed having a shallow water table within the root zone was small and restricted to lowlands near stream channels and/or zones with breaks in land surface slope from steep to gentle. GW ET began as early as June (during dry years) or as late as August (during wet years) generally peaking in September and continuing through the fall unless there was precipitation that wet the SZ and shifted ET back to SZ ET. GW storage was replenished during the wet snowmelt season (positive GW ΔS) through recharge, with greater replenishment during wet years. GW storage decreased (negative GW ΔS) through the late summer and winter due to GW ET, seepage to the land surface (spring flow), and discharge to the stream. This resulted in seasonal fluctuations in the total watershed GW storage (Figure 9a) with an annual peak during the snowmelt season followed by a gradual decrease due to drainage and ET of GW from the watershed during the dry season. Annual watershed GW storage was replenished during wet years (recharge > drainage + ET) and depleted during dry years (drainage + ET > recharge).

The changes in monthly watershed fluxes caused by 4 m of stream incision (Figure 8b) were seasonal and relatively small compared to the magnitude of fluxes within the entire watershed (Figure 8a). Incision resulted in less streamflow during the wet season (negative streamflow change in Figure 8b) and a greater increase in GW storage (positive change in GW ΔS) especially for wet years (WY 82, 83, and 86) suggesting that during the snow melt season some water that flowed to the stream in RCnat became GW recharge in RCinc4m. Incision resulted in more streamflow during the dry season (positive streamflow change) accompanied by less SZ and GW ET and more depletion of GW storage (negative change in GW ΔS). In the subsequent wet season (during wet years), incision-induced GW recharge replenished the GW storage lost during the dry season.

The net effect of the seasonal changes can be seen by summing monthly changes for each simulated water year (Figure 8c). During wet years (e.g., WY 82 and 83), the annual watershed streamflow for RCinc4m is

simulation but were not always of the observed magnitude. Simulated late summer base flows were similar in magnitude to those observed in Sagehen (17% average difference).

Allen-Diaz [1991] documented water-table-depth patterns in Sagehen meadows. She observed that depths were shallowest during the snow melt season and deepest during late summer. Observed depths were <25 cm throughout the year in the wet meadow areas, and ranged from 50 to 85 cm in the driest meadow areas. Similar patterns are seen in the RCnat results with water table depths in the wet upper meadow (Figure 7a) at or within 0.5 m of the land surface throughout the year. The drier lower meadow (Figure 7b) was not saturated for as long a period of time during the snow melt season and the water table depth reached a maximum of 1 m.

3.1. Effect of Stream Incision on Watershed Streamflow, ET, and GW Storage

RCnat monthly rates of watershed streamflow, SZ ET, GW ET (UZ ET was negligible), and GW storage change (GW ΔS) illustrate

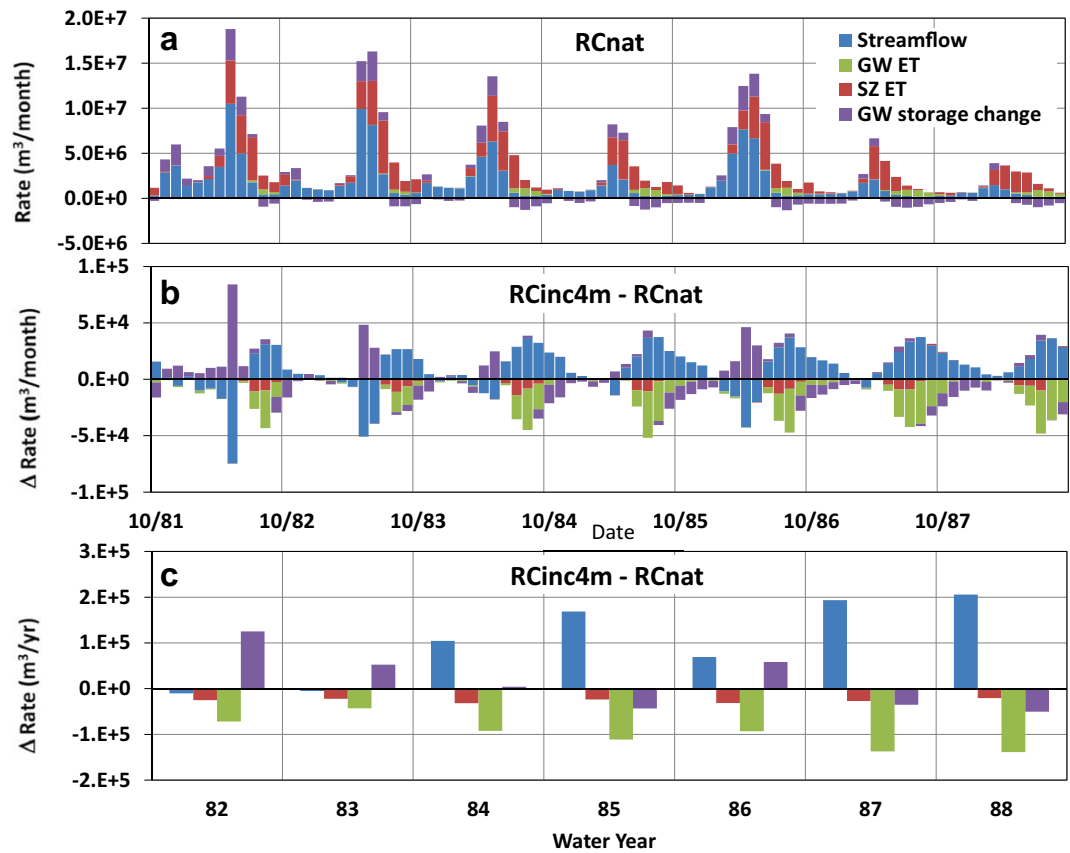


Figure 8. (a) Watershed (WS) streamflow, soil zone (SZ) and groundwater (GW) evapotranspiration (ET), and GW storage change (GW ΔS) for the reference case natural stream channel simulation; (b) the monthly change in watershed fluxes caused by 4 m of stream channel incision (positive values are increases, negative values are decreases); and (c) the net annual change in watershed fluxes caused by 4 m of incision.

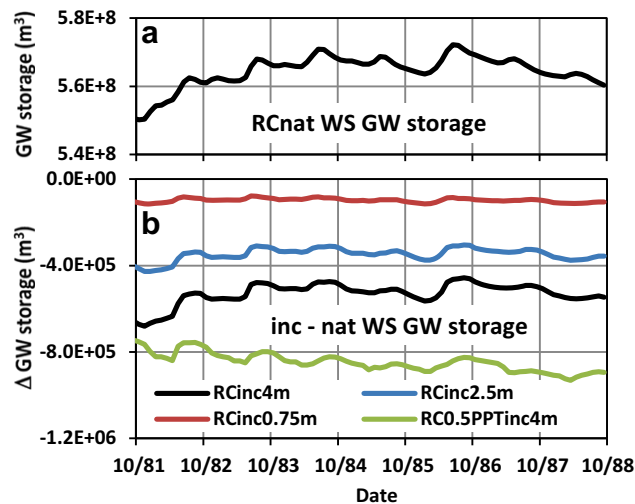


Figure 9. (a) Reference case (RC) total watershed (WS) groundwater (GW) storage for natural conditions and (b) the change in WS GW storage (inc - nat) caused by 0.75, 2.5, and 4 m of stream channel incision for the RC, and 4 m of channel incision for the reduced precipitation scenario (RC0.5PPT).

relatively unchanged from RCnat because the greater streamflow during the dry season is offset by less streamflow during the wet season, and there is a larger increase in GW storage. However, during dry years (e.g., WY 87 and 88) incision results in larger annual streamflow with the source of this additional flow being mainly captured ET and loss of GW storage. The change in water flux for RCinc4m relative to RCnat flux ranged from -0.02% (WY 83) to $+3.0\%$ (WY 88) for streamflow; -0.11% (WY 83) to -0.24% (WY 87) for SZ ET; -4.6% (WY 84) to -6.2% (WY 82) for GW ET; and 1.4% (WY 86) to -1.3% (WY 88) for GW ΔS .

The effect of incision depth on watershed fluxes was examined using the annual difference (compared to RCnat) in the rates of watershed streamflow,

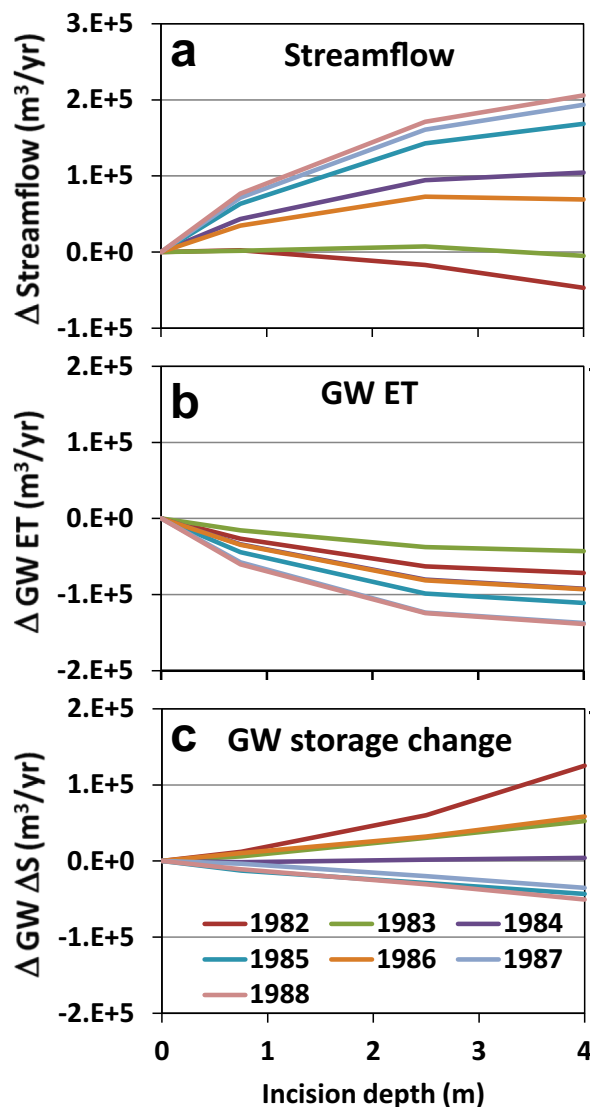


Figure 10. Annual incision-induced change in RC (a) streamflow, (b) ground-water evapotranspiration (GW ET), and (c) GW storage change as a function of incision depth (positive values represent an increase and negative values a decrease).

during wet years because wet season incision-induced recharge was greater than incision-induced GW storage depletion. In dry years, the opposite was true and there was more depletion of GW storage in the incised cases than in RCnat. Thus, the net long-term change in GW storage caused by incision will depend on the proportion of wet and dry years.

3.2. Effect of Stream Incision on the Meadow Zone

A sub-basin of the RCnat watershed model encompassing the meadows (i.e., the meadow zone) was examined in detail to illustrate the effect of stream incision on meadow hydrology. Late spring RCnat water table elevation and depth (Figures 11a) in the meadow zone show that valley topography controls the water table, with GW flowing toward the stream network. Water table depths were within 2 m of the land surface in the upper and lower meadow areas, and also at the upslope meadow margins where there was a break in land surface slope and a transition from higher K soil/weathered bedrock to the lower K meadow surface. These were areas of GW leakage to the land surface (as seeps or springs) that contributed flow to the wet

GW ET, and GW ΔS caused by 0.75, 2.5, and 4 m of incision (Figure 10). The annual incision-induced increase (during dry years, e.g., WY 87 and 88) and decrease (during wet years, e.g., WY 82 and 83) in watershed streamflow becomes more pronounced with deeper stream incision. The rate of incision-induced decrease in GW ET (greater during dry years) decreases as the incision depth increases because the water table eventually falls below the root zone and no additional GW ET can be captured. During wet years, there is a relatively large incision-induced increase in GW ΔS due to enhanced GW recharge, but the rate of decrease in GW ΔS during dry years does not change appreciably with incision depth because it is controlled by the rate at which water can drain from the system (i.e., meadow and bedrock hydraulic properties).

The effect of incision depth on seasonal GW storage dynamics can be seen by examining the change in volume of GW stored in the watershed ($\Delta GW S$), relative to RCnat, for RCinc0.75m, RCinc2.5m, and RCinc4m (Figure 9b). The negative $\Delta GW S$ caused by incision became more pronounced with greater incision depth due to increased water table lowering. The seasonal fluctuations in $\Delta GW S$ indicate that the incised watershed underwent more GW storage replenishment during the wet season and more GW storage depletion during the dry season compared to RCnat. This dynamic GW storage effect becomes more pronounced as incision depth increases as illustrated by the increased amplitude of seasonal fluctuations. Annually, there was more replenishment of GW storage in the incised cases than in RCnat

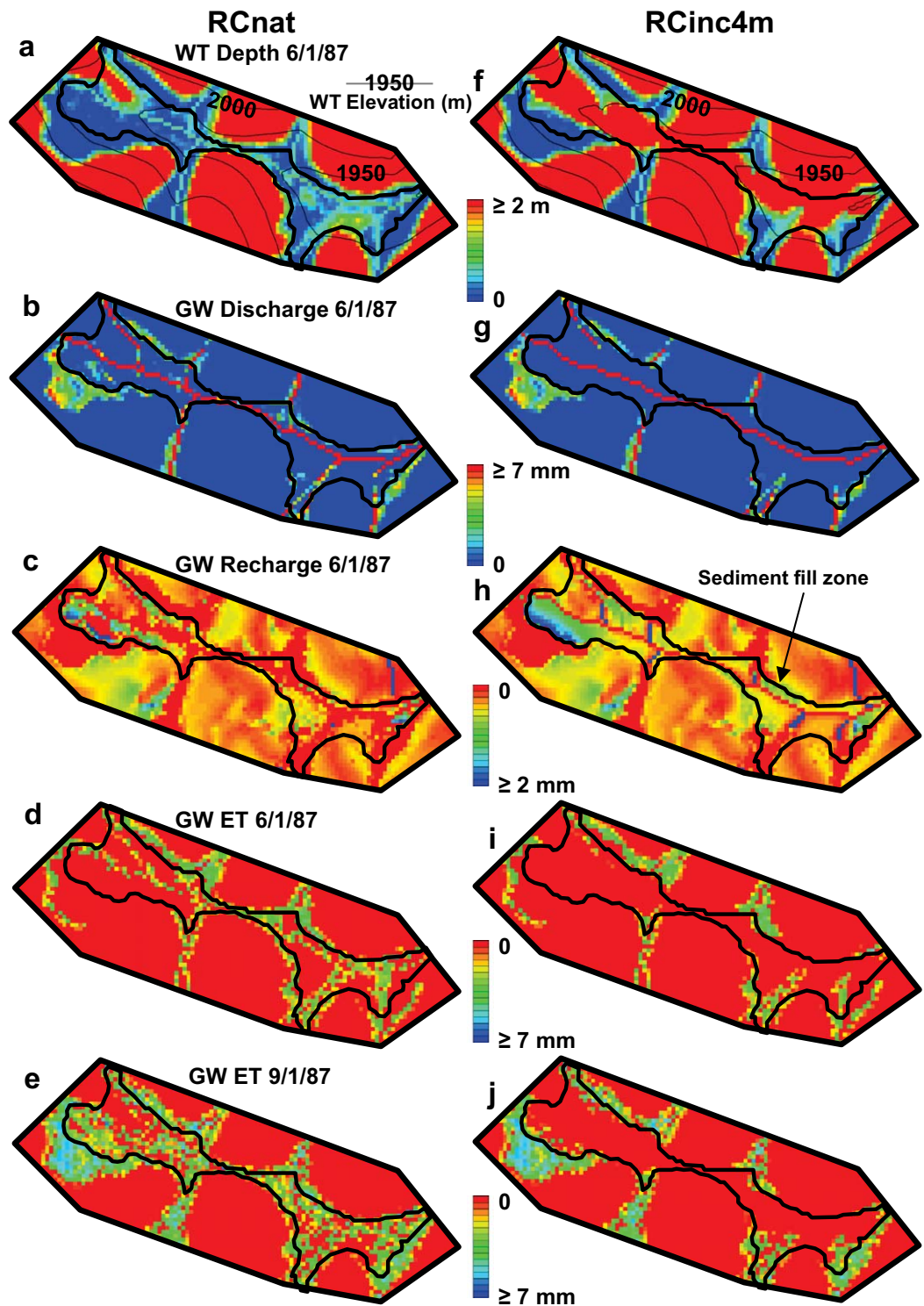


Figure 11. Meadow zone maps of reference case natural (RCnat) and 4 m incised (RCinc4m): (a and f) water table depth and elevation; (b and g) groundwater (GW) discharge; (c and h) GW recharge; and (d, e, i, and j) GW evapotranspiration (ET).

meadows. Throughout the year GW discharged to the stream network, and in the wet season GW also seeped to the land surface (Figure 11b). This occurred at the upslope margins of the meadow and also within parts of the meadow that were fully saturated. GW recharge occurred in areas of the meadow where

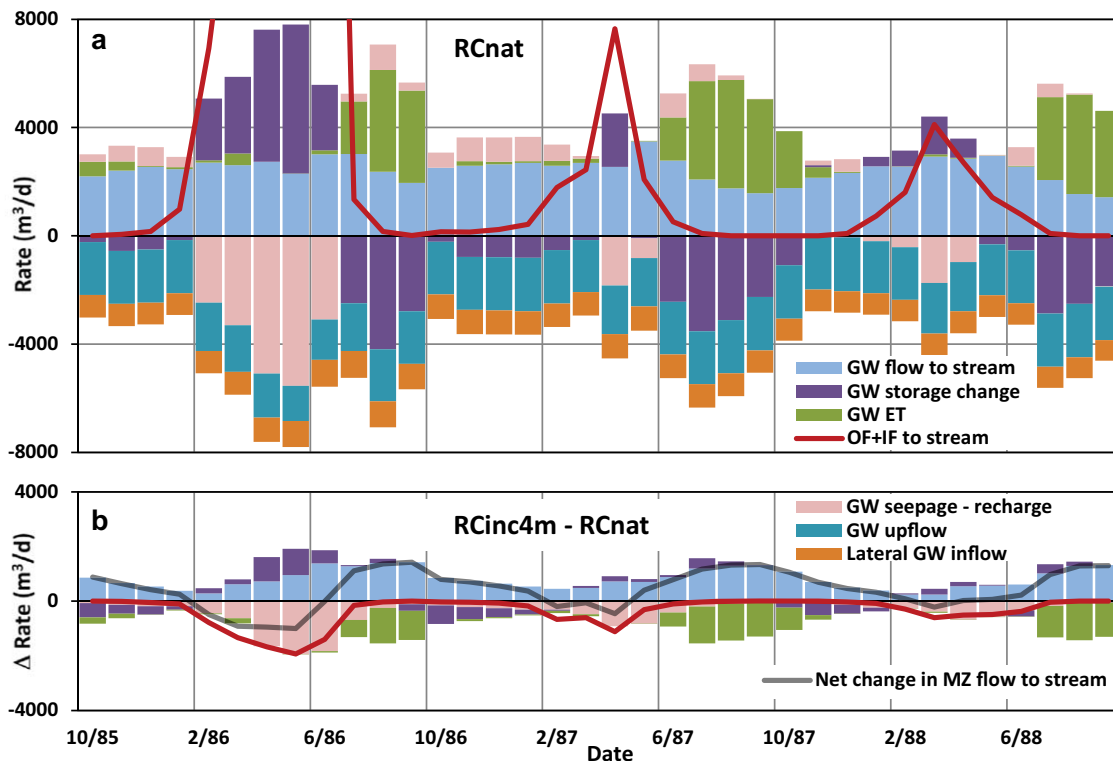


Figure 12. Reference case (a) natural meadow zone (MZ) groundwater (GW) and overland flow + interflow (OF + IF) fluxes and (b) change in meadow fluxes caused by 4 m of stream channel incision.

the water table was below the land surface (Figure 11c). By late summer (not shown), there was no GW seepage to the land surface and no GW recharge to the meadow, although there was still GW discharge to the stream. During the wet season, the meadow SZ remained wet due to inputs from hillslope OF+IF, local snowmelt, and GW leakage to the land surface, and SZ ET dominated. GW ET from the saturated zone occurred only on the margins of the meadows where the water table was below the surface yet within the root zone (Figure 11d). However, by late summer the water table dropped and the SZ dried out resulting in a shift to GW ET within the meadow areas (Figure 11e) at rates ranging from 0 to 7 mm/day depending on water table depth and root depth.

Stream incision and the consequent lowering of stream stage caused water table levels to fall in the zone adjacent to the stream channel (Figure 11f), resulting in less GW seepage to the land surface (Figure 11g), more GW recharge (Figure 11h) in the spring, and less GW ET (Figures 11i and 11j). The water table drop in the meadow due to 4 m of stream incision was greatest near the stream (Figure 7), decreased with distance from the stream and remained relatively unchanged at the hillslope-meadow contact where there was a constant source of upslope water flowing into the meadow area that was not affected by the stream incision (e.g., 280 m from stream in the lower meadow, Figure 7b). Thus, water levels in the meadow were controlled by the stream stage in the area adjacent to the stream, and by the contrast in bedrock/meadow hydraulic properties at the meadow margins distant from the stream for both natural and incised conditions. Only in the zone in between did water levels fluctuate quite differently for natural and incised conditions (e.g., 120 m in the upper meadow, 160 m in the lower meadow, Figures 7a and 7b, respectively). This interior zone of the meadow underwent larger amplitude water table fluctuations for incised conditions than for natural conditions due to the greater GW recharge in the spring and the longer period of WT drop through the fall and winter.

A GW budget analysis was conducted to illuminate the seasonal and dynamic nature of the meadow zone. GW can enter the meadow zone via lateral GW inflow, deep GW upflow and GW recharge (negative rates in Figure 12a). The inflows are balanced by GW outflows via GW seepage to the land surface, GW ET, and GW

flow to the stream (positive rates in Figure 12a). GW is stored in the meadow zone when inflows exceed outflows (positive GW ΔS in Figure 12a), and GW is drained from the meadow zone when outflows exceed inflows (negative GW ΔS in Figure 12a). The WY 86 to 88 RCnat GW budget (Figure 12a) showed that GW inflow from the adjacent bedrock (lateral GW inflow and deep GW upflow) was relatively steady compared to other fluxes. However, there was a small decrease in lateral GW inflow during the dry season, and a small decrease in deep GW upflow during the wet season when stream stage was high. During the wet season, GW was recharged (negative GW seepage – recharge in Figure 12a) by local snowmelt and OF+IF entering the area from adjacent hillslopes, resulting in an increase in GW storage (positive GW ΔS). During the dry season, GW continued to seep to the land surface at meadow margins and was not offset by meadow GW recharge (positive GW seepage – recharge), OF+IF to the stream ceased, and GW ET was active resulting in a decrease in GW storage (negative GW ΔS). As a result of these seasonal GW balance changes, meadow zone GW flow to the stream decreased during wet season peak streamflow, rebounded following peak streamflow, decreased during the summer period of active GW ET, and rebounded when GW ET diminished in the fall.

Stream incision (Figure 12b) resulted in a negligible change in GW lateral inflow and deep upflow but induced more GW recharge during the wet season (negative change in GW seepage – recharge). This resulted in less OF+IF to the stream and a larger increase in GW storage (positive change in GW ΔS). Incision also caused a decrease in GW ET (i.e., captured GW ET) during the summer and early fall, followed by increased drainage from GW storage (negative change in GW ΔS) during the rest of the dry season. These changes in GW fluxes contributed to an increase in GW flow to the incised stream that ranged from 8% (3/88) to 92% (9/88) of the natural GW flow to the stream in the meadow zone. However, the net flow to the stream (the sum of GW flow and OF+IF) from the incised meadow area was less than the natural flow to the stream in the wet season because of the decrease in OF+IF (Figure 12b). Incision-induced changes in the meadow propagated to the surrounding bedrock and hillslope areas. For example, on 1 September 1987, 80% of the GW ET reduction caused by stream incision and water table lowering occurred in the meadow zone and 20% occurred on the adjacent hillslope margins.

4. Modified Scenarios' Results

The general seasonal trends in watershed and meadow zone water fluxes for the modified scenarios were similar to those of the RC, and the meadow reach of the stream remained gaining throughout the year for all scenarios. Therefore, for brevity, only select simulation results are shown (Figures 13 and 14) and compared to the RC.

The results of the modified hydraulic conductivity scenarios demonstrated that the simulated occurrence and extent of natural meadows, as indicated by shallow water table areas (Figures 13a–13d), was affected by the contrast between bedrock and meadow K. Bedrock K controlled the rate of inflow of water into the meadow zones, and meadow K influenced the ease with which these inflows were transmitted through the meadow to the stream. Large meadow areas extending from the hillslope to the stream channel in the valley floor developed when meadow K was less than near-surface bedrock K (RCnat, M–nat and BR+nat in Figures 11a, 13a, and 13c, respectively) because bedrock and hillslope inflows maintained a shallow water table at the bedrock/meadow contact. When bedrock K was less than meadow K, meadow areas tended to be smaller, closer to the stream, and farther from the hillslope margin (M+nat and BR–nat in Figures 13b and 13d, respectively) because the rate of inflow from the bedrock was not sufficient to maintain a shallow water table at the bedrock/meadow contact. The areal extent of meadow water table drop in response to stream incision was sensitive to both meadow and bedrock hydraulic properties. The width of the zone adjacent to the stream that experienced an increase in WT depth due to stream incision was narrower when meadow K was smaller (M–inc4m, Figure 13e). The influence of stream incision on meadow water table depth extended farther from the stream when meadow K was larger (M+inc4m, Figure 13f), because the larger K meadow had a flatter water table. The width of the impacted zone was narrower for the BR+inc4m scenario (Figure 13g) than RCinc4m (Figure 11f) because of greater bedrock inflow to the meadow zone. The largest and most extensive impact of stream incision was observed in the BR– case (Figure 13h) where the entire meadow was lost as a result of stream incision.

The magnitude of incision-induced change in annual watershed streamflow, ET and GW ΔS (Figures 14a–14d) was also influenced by hydraulic properties, with the influence being larger during the dry years

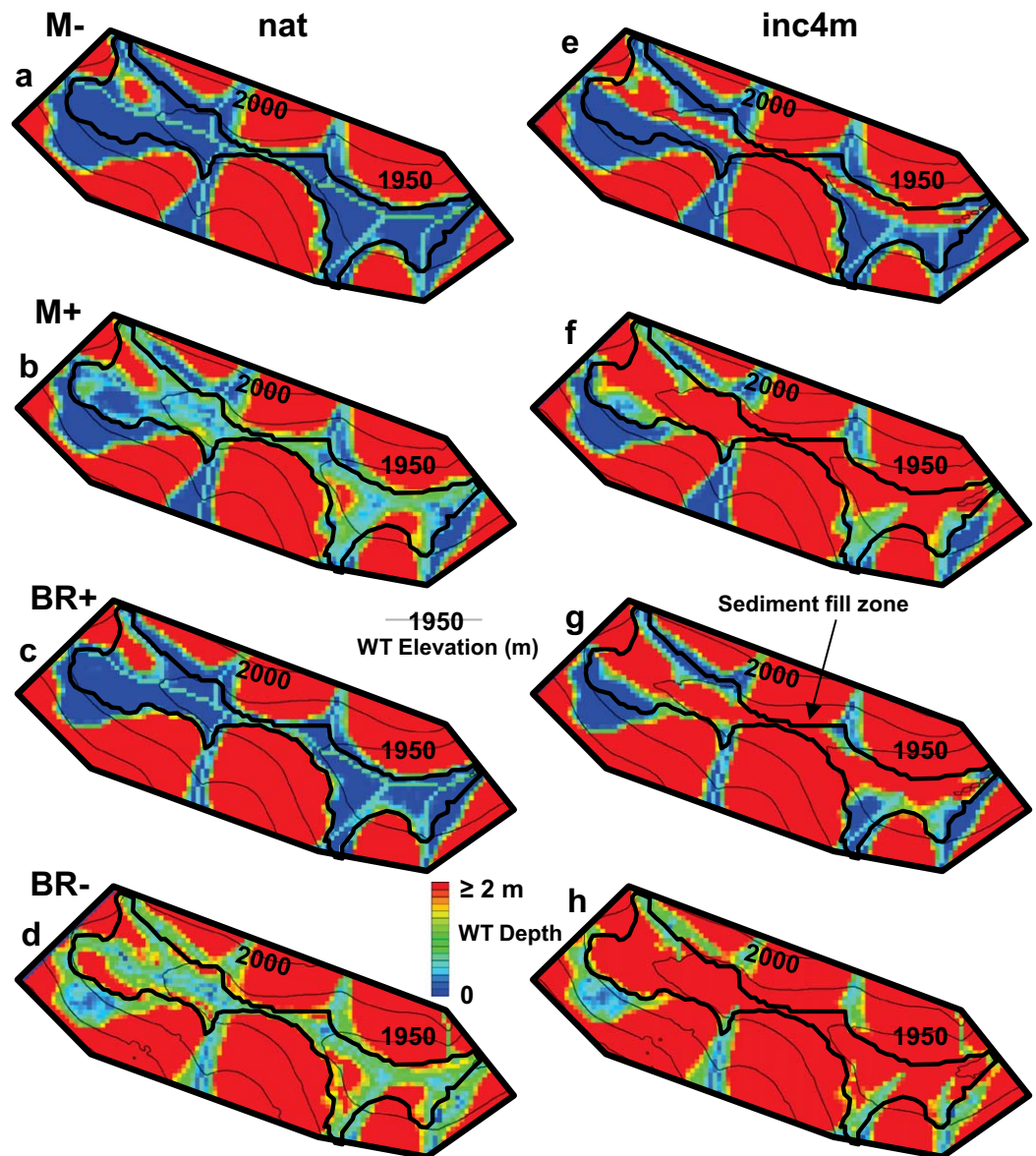


Figure 13. (a–d) Natural and (e–f) 4 m incised water table (WT) depths and elevations on 1 June 1987 for the modified hydraulic conductivity scenarios (M–, M+, BR+, and BR–).

(WY87 and 88) than during the wet year (WY88). The magnitude of streamflow increase depended on the ET available for capture and the GW storage dynamics. The RCinc4m, M–inc4m, and BR+inc4m wetter meadow scenarios all experienced a capture of both SZ ET and GW ET (Figures 8c, 14a, and 14c) resulting in larger increases in streamflow than for scenarios M+inc4m and BR–4m (Figures 14b and 14d). The decrease in GW ET was smallest in the BR–inc4m scenario (Figure 14d) because the BR–nat water table in the meadow was already below the root depth in some areas (Figure 13d), so the additional water table drop as a result of incision did not have as much impact on GW ET. The magnitude of annual watershed GW ΔS caused by incision was greater for the larger K scenarios (M+inc4m and BR+inc4m). Consequently, incision-induced streamflow increase was greatest for the BR+inc4m case, relatively similar for the RCinc4m, M–inc4m, and M+inc4m scenarios, and the least for the BR–inc4m scenario.

Comparing the modified K scenarios, natural summer meadow zone fluxes (Figures 14h–14k) to RCnat (Figure 12a) illustrates the influence of bedrock and meadow K on meadow hydrology. Larger bedrock K (BR+nat) resulted in more lateral and deep GW inflow, more GW seepage to the meadow surface (positive

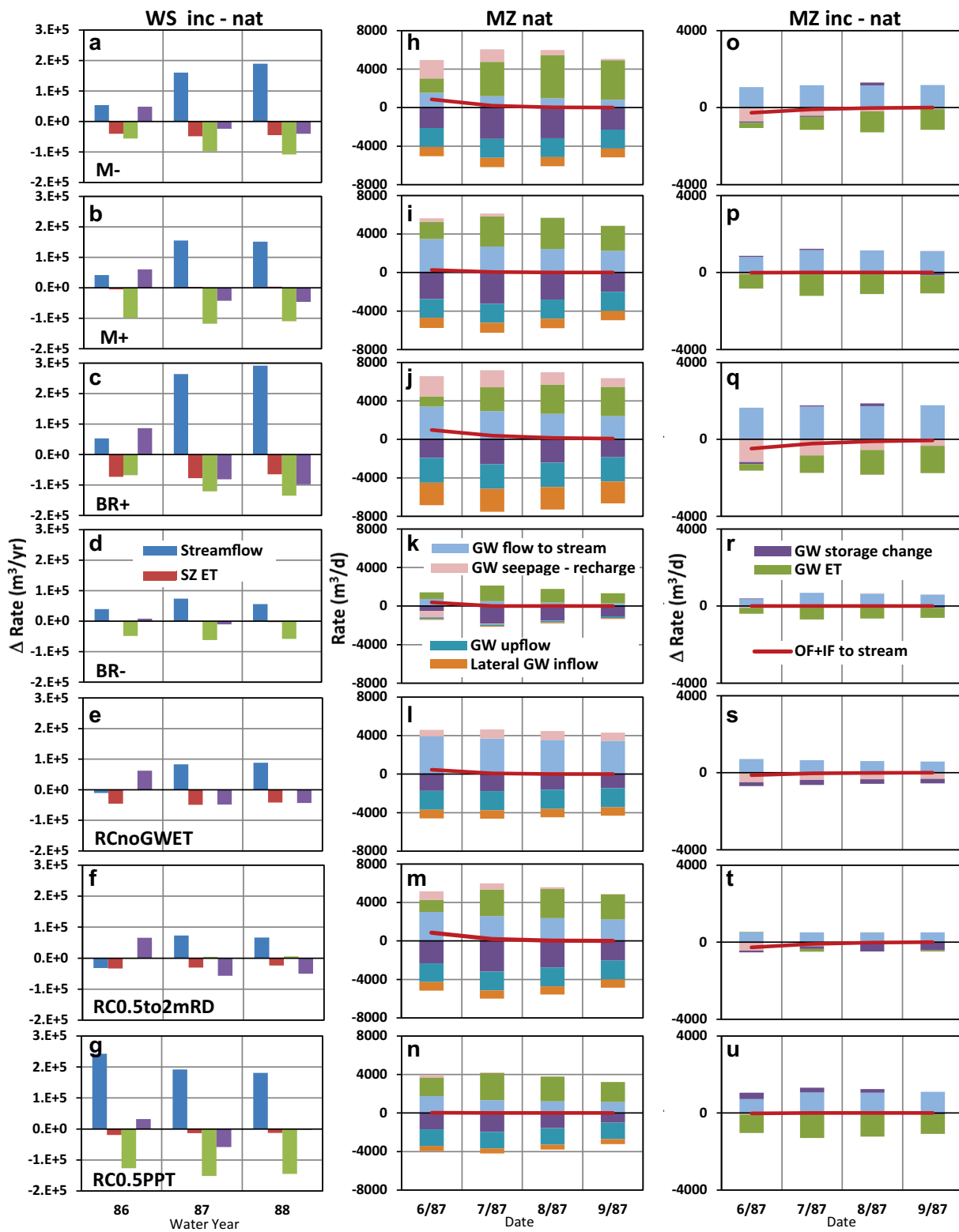


Figure 14. (a–g) Watershed (WS) change in streamflow, SZ ET, GW ET, and GW storage caused by 4 m of stream incision; (h–n) meadow zone (MZ) natural water budget; and (o–u) MZ change in water budget caused by 4 m of stream incision for the modified scenarios.

GW seepage – recharge), and less GW ET (because of the wetter SZ), and consequently more GW flow to the stream (Figure 14j). Smaller bedrock K (BR–nat) resulted in little GW inflow to the meadow zone, no GW seepage to the land surface and net GW recharge in June, reduced GW ET because of the deeper water table, and consequently less GW flow to the stream (Figure 14k). When bedrock K was unchanged, smaller meadow K (M–nat) resulted in more GW seepage to the meadow surface, more GW ET and less GW flow to the stream, with the opposite occurring for larger meadow K (M+). For all modified K scenarios, stream incision resulted in increased dry season GW flow to the stream within the meadow zone (Figures 14o–14r) resulting mainly from captured GW ET in all scenarios (negative change in GW ET) plus induced GW recharge (negative change in GW seepage – recharge) in the wetter meadow scenarios (M–inc4m and BR+inc4m).

The results from the RC and modified K scenarios illustrate the importance of GW ET in watersheds and meadows, especially with respect to the impact of stream incision on dry season streamflow. Furthermore, the RCnoGWET scenario resulted in less than half the annual incision-induced watershed streamflow increase observed in the RC simulation during dry WY 87 and 88, and an incision-induced decrease in annual streamflow during wet WY86 (Figure 14e). Compared to RCnat, RCnoGWETnat underwent less dry season GW ΔS decrease, because GW was not removed by ET, and greater GW flow to the stream (Figure 14l). The RCnoGWETinc4m incision-induced increase in meadow GW flow to the stream (Figure 14s) was 69% smaller than in the RC. The source of the extra GW flow to the stream was induced GW recharge and increased drainage from GW storage (negative change in GW ΔS). Similarly, postincision GW ET was relatively unchanged in the RC0.5to2mRD scenario, a simplified representation of postincision vegetation shift to deeper rooted trees, shrubs, and/or sagebrush in the meadow (Figures 14f and 14t). Consequently, the incision-induced change in streamflow was similar to that for the RCnoGWET scenario. The incision-induced streamflow increase was small and resulted from induced GW recharge (early in the dry season) and increased GW drainage from storage.

Reducing the RC precipitation (RC0.5PPT scenario) resulted in a deeper WT, drier SZ, and drier unsaturated zone compared to the RC. Consequently, RC0.5PPTnat experienced a larger fraction of GW ET relative to SZ ET than RCnat, and the drier unsaturated zone resulted in less infiltration and GW recharge and more OF+IF during the wet season. Thus, unlike other scenarios, stream incision resulted in an increase in annual watershed streamflow during wet WY86 that was comparable to that of dry WY87 and 88 (Figure 14g). The RC0.5PPTnat meadow zone had less GW inflow and less GW ET compared to RCnat (Figure 14n). Similar to the RCinc4m, RC0.5PPTinc4m showed an increase in GW flow to the stream that was mainly due to captured GW ET (Figure 14u). However, in contrast to other scenarios, incision caused an increase in meadow zone GW storage (positive change in GW ΔS) due to less removal of GW by ET. This scenario also differed from the RC in that the watershed decrease in GW storage caused by stream incision (Figure 9b) showed a continuous downward trend during the simulation period indicating that GW storage dynamics for this simulation were different than for the RC. Unlike the RCinc4m scenario, wet years in the RC0.5PPTinc 4 m scenario did not generate enough incision-induced GW recharge to offset the incision-induced GW storage lost during dry years. This suggests that watersheds having incised meadows in drier climates may slowly lose GW storage over time.

5. Comparison of Model Results to Previous Work

The GSFLOW model represents many watershed processes; however, it also includes many simplifications and assumptions. Confidence in the model results can be gained by comparison to field observations and previous modeling efforts. The simulated natural stream channel water table depth distributions for the RC and modified K scenarios (Figures 11 and 13) illustrated that influx of GW into meadow areas with relatively low K leads to shallower water tables at the meadow/hillslope margin, whereas, relatively higher K meadows have shallower water tables near the stream in accordance with the findings of *Loheide et al.* [2009]. The seasonal patterns of simulated water table fluctuations for natural and incised conditions (Figure 7) correspond to observations in real meadows. Under natural stream channel conditions, water tables are generally at a minimum during late summer and early fall [Wood, 1975; Allen-Diaz, 1991; Loheide and Gorelick, 2007] with water table rise starting in the fall when ET decreases. In the RC scenario, stream channel incision extended the period of water table decline into the late fall and winter (Figure 7) because of continued GW

drainage from the meadow driven by the lowered stream stage and reflected in GW storage decrease in the meadow zone (Figure 12b). Simulated incised water tables rose in response to GW recharge during the wet season. Observed water tables in Coyote Flat, a 3 m incised location within the Last Chance watershed, California [Loheide and Gorelick, 2007] showed the same trends seen in the simulated water table hydrographs in that water table levels declined through the fall and winter and rose during the spring snow melt.

Lowry and Loheide [2010] documented the importance of additional root water uptake made available by shallow GW conditions and termed this the GW subsidy. They showed that the GW subsidy was important and depended on meadow hydraulic properties, the rate of water table decline, and the root depth. Despite the simplified representation of ET processes in GSFLOW, GW ET is analogous to the GW subsidy. Simulated watershed and meadow zone fluxes illustrate the importance of GW ET during the summer and early fall when the SZ is dry (Figures 8 and 12). GW ET results in greater water table drop and base flow decline through the summer and early fall. These model results confirm the potential importance of root water uptake from shallow GW and demonstrate the mechanisms by which stream incision may result in a decrease in GW ET (Figures 8, 12, and 14). The magnitude of GW ET is dependent on system hydraulic properties, as demonstrated in Lowry and Loheide [2010], as well as vegetation distributions and stream incision. The simulated summer GW ET rates ranged between 0 and 7 mm/day and are in good agreement with field estimates in the northern Sierra Nevada that have ranged from 0.2 to 7.2 mm/day [Loheide and Gorelick, 2005, 2006; Hammersmark et al., 2008, 2009; Lowry and Loheide, 2010].

In contrast to the intermittent stream systems modeled by Hammersmark et al. [2008] and Ohara et al. [2013], the stream continued flowing in the meadow throughout the year for all simulated scenarios considered in this study. The findings of this study regarding changes in watershed and meadow area water fluxes in response to stream incision are in good agreement with the simulations of Hammersmark et al. [2008] in Bear Creek meadow. Similar to this study, their field work and modeling documented that returning the incised stream channel to natural conditions (meadow restoration) raised GW levels, increased GW stored in the meadow; decreased annual runoff, decreased base flow within the restored meadow (but increased base flow downstream of the meadow), and increased ET. However, unlike their study, our model results did not predict a decrease in the magnitude of flood peaks for the restored stream channel, or the downstream base flow increase. In contrast to Hammersmark et al. [2008], the Last Chance Creek, California, meadow restoration model of Ohara et al. [2013] indicated that restoration enhanced dry season base flow by 10–20%. They concluded that ET changes (based on changes in soil moisture availability) caused by incision were small. Hammersmark et al. [2008] and Ohara et al. [2013] both predicted that restoration and increased overbank flow would lead to increased meadow recharge and decreased flood flow peaks, a phenomenon not observed in our simulated scenarios. In all scenarios the stream remained gaining through the meadow, even during high flow events, and never directly recharged GW because the stream stage never exceeded the GW level; the source of meadow GW recharge was bedrock GW inflow and hillslope OF+IF to the meadow. The simulated natural meadows became flooded during snowmelt season due to large hillslope influxes and rising water tables, rather than overbank flooding. Stream incision lowered the water table and induced GW recharge in the meadow and consequently, less OF+IF to the stream. Hammersmark et al. [2008] and Ohara et al. [2013] results suggest that streamflow response to incision may be different in wider, flatter, and drier meadow systems where GW recharge by overbank flooding is the dominant GW recharge mechanism.

These differences in model predictions of the effect of stream incision on streamflow suggest that there is a spectrum of streamflow response to meadow stream-channel incision. In relatively wet meadow systems and meadows with perennial streams that are fed by inflows from the adjacent hillslopes and GW from the bedrock aquifer, stream channel incision can induce GW recharge, and result in less wet season streamflow and more dry season streamflow. The magnitude of dry season streamflow increase is very sensitive to the change in GW ET; the increase will be small if GW ET change is small. In contrast, stream incision in relatively dry meadows may decrease overbank flows, resulting in larger wet season streamflow and less GW recharge. Depending on the relative change in GW recharge and ET this may or may not lead to an increase in dry season streamflow.

6. Discussion and Conclusions

In undisturbed montane watersheds, wet meadow conditions develop when bedrock transmits GW flow to the meadow at a rate sufficient to maintain high water tables in the meadow sediments (e.g., RC, BR+, M–

scenarios). Under these conditions, meadow areas can extend from the bedrock/meadow sediment contact to the stream. Water tables are deeper and meadow extent is smaller when there is less bedrock GW flow to the meadow (e.g., BR− scenario), and when meadow K is larger (e.g., M+ scenario) because the water table in the meadow is flatter. In these cases, meadows are restricted to areas adjacent to the stream. Meadows with lower K sediments (RC and M− scenarios) and/or larger GW inflows from bedrock (BR+ scenario) sustain longer periods of meadow saturation and do not dry out as quickly. Wetter meadows also have more GW seepage to the land surface, and more OF+IF to the stream.

Stream channel incision, and the consequent lowering of the water table, is directly analogous to pumping and the resultant cone of depression. Thus, the concepts presented by Theis [1940], Bredehoeft *et al.* [1982], and Bredehoeft [1997] are directly applicable to understanding the change in montane meadow hydrology in response to stream incision. As Theis stated “*Under natural conditions. . . aquifers are in a state of approximate dynamic equilibrium. . . thus a new discharge superimposed upon a previously stable system . . . must be balanced by an increase in the recharge of the aquifer, or by a decrease in the old natural discharge, or by loss of storage in the aquifer, or by a combination of these.*” In the case of an incised montane meadow, a new discharge is superimposed on the natural system as a result of the lowering of the stream stage in the incised channel. Theis [1940] described a scenario, analogous to wet meadow systems, for which the potential recharge rate may be so large in wet seasons that the aquifer becomes overfull and available recharge is rejected because the water table stands at or near the surface in the recharge area. Lowering of the water table (by pumping or stream incision) in such a system will increase GW recharge, decrease GW discharge to the land surface, and decrease ET resulting in increased GW flow through the system to a well in the case of a pumped system, or to the incised stream in the case of a meadow system. During the wet season, when GW storage is replenished (especially during wet years), OF+IF may decrease as a result of stream incision more than GW flow to the stream increases, resulting in a net decline in meadow flow to the stream. However, during the dry season when there is no OF+IF and only GW flow from the meadow to the stream, stream incision will cause an increase in meadow flow to the stream. The magnitude of increase will depend on the amount of: captured ET, net-induced recharge (induced GW recharge + captured GW seepage), and GW storage decrease.

The response of a watershed to stream incision is influenced by the meadow and bedrock hydraulic conductivity. In incised low K wet meadows (M− scenario), the zone of substantial water table drop is limited to the area adjacent to the stream; however, in drier meadows (BR− and, M+ scenarios) the water table drop can extend to the bedrock/meadow sediment contact. In all simulations, stream incision resulted in an overall watershed loss of GW storage due to the water table drop in the watershed. The GW storage loss and seasonal fluctuations caused by incision became more pronounced as incision depth increased, and were dependent on wet season precipitation. During wet years, the GW storage loss caused by stream incision during the dry season was replenished by snowmelt-season GW recharge. However, dry-year snowmelt-season GW recharge could not fully replenish incision-induced GW storage loss. Thus, the long-term effect of stream incision on watershed GW storage will depend on precipitation. Incised systems that experience frequent wet years may not have long-term GW storage loss, but systems that have less precipitation (e.g., RC0.5PPT) may undergo slow, long-term GW storage loss.

All incised simulations conducted as part of this study resulted in an increase in summer base flow with the magnitude of the increase being most sensitive to the amount of captured GW ET. The change in GW ET due to incision will depend on: the extent of water table lowering; the function relating GW ET to water table depth (simplified by a linear function in the GSFLOW model); the depth of the roots; and the type of vegetation. Thus, there is considerable uncertainty in the model prediction of the magnitude of this effect. The relation between GW ET and water table depth is very complex and likely not linear, and the response of vegetation and roots to water table drop is also complex. As illustrated by the simulation assuming a transition of vegetation from grass to deep-rooted plants following incision, over the long term it may be possible for vegetation to shift to plants with deeper roots that can transpire nearly the same amount of water from the deep water table that meadow grasses could under natural conditions.

The simulations presented in this work illustrate the difference between natural systems and incised systems in relative dynamic equilibrium, but do not characterize the transitional response of the watershed as it is undergoing active stream incision or restoration. The results from a simplified, long-term simulation for the RC scenario with a steady annual precipitation function (WY85 precipitation) suggested that the

watershed flows adjusted within one year to a step change in stream incision or restoration because the system quickly achieved a new dynamic equilibrium. Summer streamflow was greatest during the year in which stream incision occurred (due to rapid decrease in meadow GW storage), and least during the year in which stream restoration occurred (due to rapid replenishment of meadow GW storage). Thus, it is conceivable a multiyear period of active stream incision could have summer flows that would be greater than the summer flow after incision stopped and the stream channel stabilized.

In conclusion, the occurrence and development of montane meadows depends on the interplay between topography, bedrock and meadow hydraulic properties, climate, vegetation, and the resultant surface and GW inflows to the meadow zone. Likewise, the susceptibility and sensitivity of meadows to stream incision is also controlled by these factors. In general, the GW fed meadow conditions considered in this study, in contrast to meadows recharged primarily by surface water overbank flooding, showed an increase in summer streamflow due to incision, with the sources of the augmented flow being a combination of: (1) reduced ET in the eroded meadow; (2) induced GW recharge; (3) drainage of GW stored in meadow and bedrock aquifers that was replenished by precipitation during wet years; and (4) drainage of GW stored in meadow and bedrock aquifers that was not replenished by precipitation during wet years. The long-term net effect of stream incision on summer streamflow and GW storage will depend on the relative magnitude of these processes in a given meadow and climate setting.

Acknowledgments

This work has been supported by the CA Department of Water Resources, USDA Forest Service, and the U.S. Geological Survey. We thank Liza Hoos (graduate student, Duke University) for her assistance with GIS analysis, and Andrew Manning (USGS) for providing well information, and Rich Niswonger (USGS) for GSFLOW support. We also thank Jim Constantz and three anonymous reviewers for their constructive comments and suggestions. The GSFLOW software used for this study is available at <http://water.usgs.gov/nrp/gwsoftware/gsflow/gsflow.html> and specific model data are available from the corresponding author.

References

- Allen-Diaz, B. H. (1991), Water table and plant species relationships in Sierra Nevada meadows, *Am. Midland Nat.*, 126, 30–43.
- Boulton, A. J. (2005), Chances and challenges in the conservation of groundwater and their dependent ecosystems, *Aquat. Conserv. Mar. Freshwater Ecosyst.*, 15, 319–323.
- Bredehoeft, J. (1997), Safe yield and the water budget myth, *Ground Water*, 35(6), 929.
- Bredehoeft, J. D., S. S. Papadopoulos, and H. H. Cooper (1982), Groundwater: The water budget myth, in *Scientific Basis of Water-Resource Management, Studies in Geophysics*, pp. 51–57, Panel on Scientific Basis of Water Resource Management, National Research Council, Natl. Acad. Press, Washington, D. C.
- Chambers, J. C., J. R. Miller, and D. Germanoski (2011), Chap. 1: Introduction and overview, in *Geomorphology, Hydrology, and Ecology of Great Basin Meadow Complexes: Implications for Management and Restoration, Gen. Tech. Rep. RMRS-GTR-258*, edited by J. C. Chambers and J. R. Miller, pp. 1–10, U.S. Dep. of Agric., For. Serv., Rocky Mt. Res. Stn, Fort Collins, Colo.
- Earman, S., J. Clark, S. Diaz, A. Manning, D. Pool, and S. Urióstegui, (2013), Investigation of methods of potential value to monitor groundwater recharge in the mountains of California, *Public Interest Energy Research (PIER) Final Proj. Rep. PIR-08-010*, California Energy Commission, Sacramento, Calif.
- Fryjoff-Hung, A. and J. H. Viers (2013), *Sierra Nevada Meadow Hydrology Assessment: Final Project Report to the USDA Forest Service Pacific Southwest Region (USFS PSW)*, 1114 ppd, Univ. of Calif., Davis, Calif.
- Hammersmark, C. T., M. C. Rains, and J. F. Mount (2008), Quantifying the hydrological effects of stream restoration in a montane meadow, northern California, USA, *River Res. Appl.*, 24(6), 735–753.
- Hammersmark, C. T., M. C. Rains, A. C. Wickland, and J. F. Mount (2009), Vegetation and water-table relationships in a hydrologically restored riparian meadow, *Wetlands*, 29(3), 785–797.
- Hammersmark, C. T., S. Z. Dobrowski, M. C. Rains, and J. F. Mount (2010), Simulated effects of stream restoration on the distribution of wet-meadow vegetation, *Restor. Ecol.*, 18(6), 882–893.
- Harbaugh, A. W. (2005), MODFLOW-2005, The U.S. Geological Survey modular ground-water model: The Ground-Water Flow Process, *U.S. Geol. Surv. Tech. Methods 6-A16*, 253 pp.
- Henson, W. R., R. L. Medina, C. J. Mayers, R. G. Niswonger, and R. S. Regan (2013), CRT: Cascade Routing Tool to define and visualize flow paths for grid-based watershed models, *U.S. Geol. Surv. Tech. Methods 6-D2*, 28 pp.
- Hill, B., and S. Mitchell-Bruker (2010), Comment on “A framework for understanding the hydroecology of impacted wet meadows in the Sierra Nevada and Cascade Ranges, California, USA” by Steven P. Loheide II et al., *Hydrogeol. J.*, 18(7), 1741–1743.
- Jackson, R. B., J. Canadell, J. R. Ehleringer, H. A. Mooney, O. E. Sala, and E. D. Schulze (1996), A global analysis of root distributions for terrestrial biomes, *Oecologia*, 108, 389–411.
- Jiang, X.-W., L. Wan, X.-S. Wang, S. Ge, and J. Liu (2009), Effect of exponential decay in hydraulic conductivity with depth on regional groundwater flow, *Geophys. Res. Lett.*, 36, L24402, doi:10.1029/2009GL041251.
- Jin, L., D. I. Siegel, L. K. Lutz, and Z. Lu (2012) Identifying streamflow sources during spring snowmelt using water chemistry and isotopic composition in semi-arid mountain streams, *J. Hydrol.*, 470–471, 289–301, doi:10.1016/j.jhydrol.2012.09.009.
- Klein, L. R., S. R. Clayton, J. R. Alldredge, and P. Goodwin (2007), Long-term monitoring and evaluation of the Lower Red River meadow restoration project, Idaho, USA, *Restor. Ecol.*, 15(2), 223–239.
- Leavesley, G. H., R. W. Lichty, B. M. Troutman, and L. G. Saindon (1983), Precipitation-runoff modeling system: User’s manual, *U.S. Geol. Surv. Water Resour. Invest. Rep. 83–4238*, 207 pp, U. S. Geological Survey, Denver, Colo.
- Leavesley, G. H., S. L. Markstrom, R. J. Viger, and L. E. Hay (2005), USGS modular modeling system (MMS): Precipitation-runoff modeling system (PRMS) MMS-PRMS, in *Watershed Models*, edited by V. Singh and D. Frevert, pp. 159–177, CRC Press, Boca Raton, Fla.
- Loheide, S. P., II, and E. G. Booth (2011), Effects of changing channel morphology on vegetation, groundwater, and soil moisture regimes in groundwater-dependent ecosystems, *Geomorphology*, 126, 364–376.
- Loheide, S. P., and S. M. Gorelick (2005), A high-resolution evapotranspiration mapping algorithm (ETMA) with hydroecological applications at riparian restoration sites, *Remote Sens. Environ.*, 98, 182–200.
- Loheide, S. P., II, and S. M. Gorelick (2006), Quantifying stream-aquifer interactions through the analysis of remotely sensed thermographic profiles and in situ temperature histories, *Environ. Sci. Technol.*, 40(10), 3336–3341.

- Loheide, S. P., II, and S. M. Gorelick (2007), Riparian hydroecology: A coupled model of the observed interactions between groundwater flow and meadow vegetation patterning, *Water Resour. Res.*, *43*, W07414, doi:10.1029/2006WR005233.
- Loheide, S. P., II, R. S. Deitchman, D. J. Cooper, E. C. Wolf, C. T. Hammersmark, and J. D. Lundquist (2009), A framework for understanding the hydroecology of impacted wet meadows in the Sierra Nevada and Cascade Ranges, California, USA, *Hydrogeol. J.*, *17*, 229–246.
- Loheide, S. P., II, R. S. Deitchman, D. J. Cooper, E. C. Wolf, C. T. Hammersmark, and J. D. Lundquist (2010), Reply to comment on “A framework for understanding the hydroecology of impacted wet meadows in the Sierra Nevada and Cascade Ranges, California, USA” by Steven P. Loheide II et al., *Hydrogeol. J.*, *18*(7), 1745–1746.
- Lord, M. L., D. G. Jewett, J. R. Miller, D. Germanoski, and J. C. Chambers (2011), Chapter 4: Hydrologic processes influencing meadow ecosystems, in *Geomorphology, Hydrology, and Ecology of Great Basin Meadow Complexes: Implications for Management and Restoration*, Gen. Tech. Rep. RMRS-GTR-258, edited by J. C. Chambers and J. R. Miller, pp. 44–67, U.S. Dept. of Agric., For. Serv., Rocky Mt. Res. Stn., Fort Collins, Colo.
- Lowry, C. S., and S. P. Loheide II (2010), Groundwater dependent vegetation: Quantifying the groundwater subsidy, *Water Resour. Res.*, *46*, W06202, doi:10.1029/2009WR008874.
- Lowry, C. S., J. S. Deems, S. P. Loheide II, and J. D. Lundquist (2010), Linking snowmelt-derived fluxes and groundwater flow in a high elevation meadow system, Sierra Nevada Mountains, California, *Hydro. Processes*, *24*(20), 2821–2833.
- Lowry, C. S., S. P. Loheide II, C. E. Moore, and J. D. Lundquist (2011), Groundwater controls on vegetation composition and patterning in mountain meadows, *Water Resour. Res.*, *47*, W00J11, doi:10.1029/2010WR010086.
- Maidment, D. R. (2002), *Arc Hydro: GIS for Water Resources*, vol. 1, ESRI Press, Redlands, Calif.
- Manning, A. H., J. F. Clark, S. H. Diaz, L. K. Rademacher, S. Earman, and L. N. Plummer (2012), Evolution of groundwater age in a mountain watershed over a period of thirteen years, *J. Hydrol.*, *460–461*, 13–28.
- Manning, C. E., and S. E. Ingebritsen (1999), Permeability of the continental crust: Implications of geothermal data and metamorphic systems, *Rev. Geophys.*, *37*, 127–150, doi:10.1029/1998RG900002.
- Markstrom, S. L., R. G. Niswonger, R. S. Regan, D. E. Prudic, and P. M. Barlow (2008), GSFLOW: Coupled ground-water and surface-water flow model based on the integration of the Precipitation-Runoff Modeling System (PRMS) and the Modular Ground-Water Flow Model (MODFLOW-2005), *U.S. Geol. Surv. Tech. Methods 6-D1*, 240 pp.
- Mast, M. A., and D. W. Clow (2000), Environmental characteristics and water-quality of Hydrologic Benchmark Network stations in the Western United States, *U.S. Geol. Surv. Circ. 1173-D*, 115 pp.
- Murray, B. R., M. Zeppel, G. C. Hose, and D. Eamus (2003), Groundwater dependent ecosystems in Australia: It's more than just water for rivers, *Ecol. Manage. Restor.*, *4*, 110–113.
- Natural Resources Conservation Service, 2011, United States Department of Agriculture. Soil Survey Geographic (SSURGO) Database. [Available at <http://soildatamart.nrcs.usda.gov>, last accessed on 2 March 2011.]
- Niswonger, R. G., D. E. Prudic, S. L. Markstrom, R. S. Regan, and R. J. Viger (2006), GSFLOW: A basin-scale model for coupled simulation of ground-water and surfacewater flow: Part B: Concepts for modeling ground-water flow with the U.S. Geological Survey MODFLOW model, paper presented at Joint 8th Federal Interagency Sedimentation and 3rd Federal Interagency Hydrologic Modeling Conference, Reno, Nevada, 2–6 April, sponsored by the Subcommittee on Hydrology of the Advisory Committee on Water Information.
- Niswonger, R. G., S. Panday, and M. Ibaraki (2011), MODFLOW-NWT, A Newton formulation for MODFLOW-2005, *U.S. Geol. Surv. Tech. Methods 6-A37*, 44 pp.
- Ohara, N., M. L. Kavvas, Z. Q. Chen, L. Liang, M. Anderson, J. Wilcox, and L. Mink (2013), Modelling atmospheric and hydrologic processes for assessment of meadow restoration impact on flow and sediment in a sparsely gauged California watershed, *Hydro. Processes*, doi: 10.1002/hyp.9821.
- Orellana, F., P. Verma, S. P. Loheide II, and E. Daly (2012), Monitoring and modeling water-vegetation interactions in groundwater-dependent ecosystems, *Rev. Geophys.*, *50*, RG3003, doi:10.1029/2011RG000383.
- Payn, R. A., M. N. Gooseff, B. L. McGlynn, K. E. Bencala, and S. M. Wondzell (2012), Exploring changes in the spatial distribution of stream baseflow generation during a seasonal recession, *Water Resour. Res.*, *48*, W04519, doi:10.1029/2011WR011552.
- Rademacher, L. K., J. F. Clark, D. W. Clow, and G. B. Hudson (2005), Old groundwater influence on stream hydrochemistry and catchment response times in a small Sierra Nevada catchment: Sagehen Creek, California, *Water Resour. Res.*, *41*, W02004, doi:10.1029/2003WR002805.
- Ratliff, R. D. (1985), Meadows in the Sierra Nevada of California: state of knowledge, *USDA For. Serv. Gen. Tech. Rep. PSW-84*, Pac. Southwest For. and Range Exp. Stn., Berkeley, Calif.
- Sanderson, J. S., and D. J. Cooper (2008), Ground water discharge by evapotranspiration in wetlands of an arid intermountain basin, *J. Hydrol.*, *351*, 344–359.
- Sylvester, A. G. (2008), Geology of the Sagehen Creek and Independence Lake Hydrologic Basins, Sierra and Nevada Counties, California, University of California, Santa Barbara. [Available at <http://www.geol.ucsb.edu/projects/tahoe/Sagehen/welcomeSage.html>.]
- Tague, C., S. Valentine, and M. Kotchen (2008), Effect of geomorphic channel restoration on streamflow and groundwater in a snowmelt-dominated watershed, *Water Resour. Res.*, *44*, W10415, doi:10.1029/2007WR006418.
- Theis, C.V. (1940), The source of water to wells: Essential factors controlling the response of an aquifer to development, *Civ. Eng.*, *10*, 277–280.
- Viers, J. H., S. E. Purdy, R. A. Peek, A. Fryjoff-Hung, N. R. Santos, J. V. E. Katz, J. D. Emmons, D. V. Dolan, and S. M. Yarnell (2013) Montane meadows in the Sierra Nevada: Changing hydroclimatic conditions and concepts for vulnerability assessment, *Cent. for Watershed Sci. Tech. Rep. CWS-2013-01*, Univ. of Calif., Davis. 63 pp.
- Weixelman, D. A., B. Hill, D. J. Cooper, E. L. Berlow, J. H. Viers, S. E. Purdy, A. G. Merrill, and S. E. Gross (2011), A field key to meadow hydrogeomorphic types for the Sierra Nevada and Southern Cascade Ranges in California, *Gen. Tech. Rep. RS-TP-034*, U.S. Dep. of Agric., For. Serv., Pac. Southwest Reg., Vallejo, Calif, 34 pp.
- Wood, S. H. (1975), Holocene Stratigraphy and Chronology of Mountain Meadows, Sierra Nevada, California, PhD. Dissertation, California Institute of Technology, Pasadena, Calif, 180 pp.